SIAM J. APPL. MATH.
Vol. 60, No. 2, pp. 503–535

SUBCRITICAL ELLIPTIC BURSTING OF BAUTIN TYPE*

EUGENE M. IZHIKEVICH†

Abstract. Bursting behavior in neurons is a recurrent transition between a quiescent state and repetitive spiking. When the transition to repetitive spiking occurs via a subcritical Andronov–Hopf bifurcation and the transition to the quiescent state occurs via double limit cycle bifurcation, the burster is said to be of *subcritical elliptic* type. When the fast subsystem is near a Bautin (generalized Hopf) point, both bifurcations occur for nearby values of the slow variable, and the repetitive spiking has small amplitude. We refer to such an elliptic burster as being of local *Bautin* type. First, we prove that any such burster can be converted into a canonical model by a suitable continuous (possibly noninvertible) change of variables. We also derive a canonical model for weakly connected networks of such bursters. We find that behavior of such networks is quite different from the behavior of weakly connected phase oscillators, and it resembles that of strongly connected relaxation oscillators. As a result, such weakly connected bursters need few (usually one) bursts to synchronize. In-phase synchronization is possible for bursters having quite different quantitative features, whereas out-of-phase synchronization may be difficult to achieve. We also find that interactions between bursters depend crucially on the spiking frequencies. Namely, the interactions are most effective when the presynaptic interspike frequency matches the frequency of postsynaptic oscillations. Finally, we use the FitzHugh–Rinzel model to evaluate how studying local Bautin bursters can contribute to our understanding of the phenomena of subcritical elliptic bursting.

Key words. subcritical elliptic burster, "sub-Hopf/fold cycle" burster, subcritical Andronov–Hopf bifurcation, double limit cycle bifurcation, Bautin bifurcation, normal form, canonical model, slow passage effect, weakly connected networks, fast threshold modulation, FM interactions, FitzHugh–Rinzel model

AMS subject classifications. 92B20, 92C20, 82C32, 58Fxx, 34Cxx, 34Dxx

PII. S003613999833263X

1. Introduction.

1.1. Bursters.

Bursting behavior in neurons is a periodic transition between a quiescent state and a state of repetitive firing; see Figure 1.1. Many mathematical models of bursters often can be written in the singularly perturbed form

$$\begin{aligned} \dot{x} &= f(x,y), \\ \dot{y} &= \mu g(x,y), \end{aligned} \tag{1.1}$$

where $x \in \mathbb{R}^m$ is a vector of fast variables responsible for repetitive firing. It accounts, e.g., for the membrane voltage and fast ion channels. The vector $y \in \mathbb{R}^k$ is a vector of slow variables that modulates the firing. It accounts for slow ion channels and currents. Small parameter $\mu \ll 1$ is a ratio of fast/slow time scales.

First, let us consider the fast subsystem $\dot{x} = f(x,y)$ alone and treat y as a bifurcation parameter. This is a standard approach known as dissection of bursting (Rinzel and Lee (1987)). The silent phase of burster corresponds to x being at an equilibrium. The repetitive spiking corresponds to x being on a limit cycle; see Figure 1.2.

*Received by the editors January 19, 1998; accepted for publication (in revised form) February 4, 1999; published electronically January 11, 2000.
http://www.siam.org/journals/siap/60-2/33263.html
†Center for Systems Science and Engineering, Arizona State University, Tempe, AZ 85287-7606 (Eugene.Izhikevich@asu.edu, http://math.la.asu.edu/~eugene).

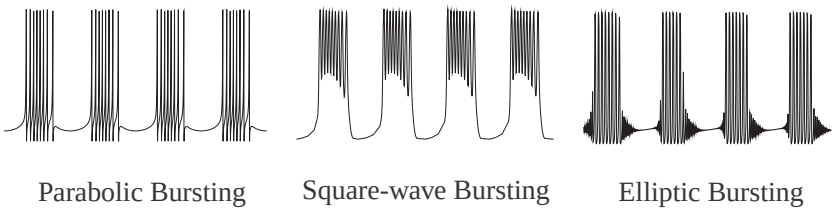

FIG. 1.1. *Major types of bursters* (*from Hoppensteadt and Izhikevich* (1997)). *Reprinted with permission from Springer-Verlag.*

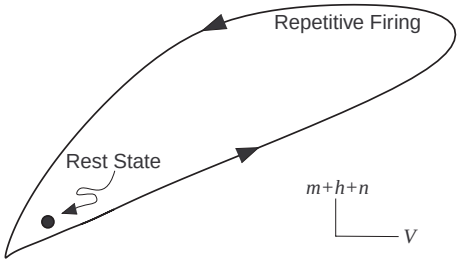

FIG. 1.2. *Projection of a periodic solution* ($I = 7$) *and a quiescent solution* ($I = 0$) *of the Hodgkin–Huxley model on the plane* $(V, m + h + n)$.

As y changes slowly, the attractors of the fast subsystem bifurcate. Among many possible bifurcations there are two that define the type of burster:

- The bifurcation of equilibrium that corresponds to transition from rest state to repetitive firing. This bifurcation determines how the repetitive firing appears.
- The bifurcation of the limit cycle that corresponds to transition from repetitive spiking to rest state. This bifurcation determines how the repetitive firing disappears.

A partial classification of bursters based on these bifurcations is provided by Wang and Rinzel (1995), Bertram et al. (1995), and Hoppensteadt and Izhikevich (1997, section 2.9.5). A complete classification is provided by Izhikevich (2000). For example, when both bifurcations are of saddle-node on limit cycle type, the burster is said to be parabolic. When the rest activity disappears via saddle-node bifurcation and the repetitive firing disappears via saddle separatrix loop bifurcation, the burster is said to be of square-wave type.

When the quiescent state loses stability via Andronov–Hopf bifurcation and repetitive firing disappears via double limit cycle bifurcation or another Andronov–Hopf bifurcation, the burster is said to be *elliptic*. A distinctive feature of elliptic bursting is that the frequency of emerging and ceasing spiking is nonzero, while the amplitude may be small.

Since Andronov–Hopf bifurcation may be subcritical or supercritical, there are many subtypes of elliptic bursters. An elliptic burster is said to be *supercritical* or "Hopf/Hopf" when both Andronov–Hopf bifurcations are supercritical (Izhikevich (1998)). An elliptic burster is said to be *subcritical* or "sub-Hopf/fold cycle" when the rest activity loses stability via subcritical Andronov–Hopf bifurcation, and the repetitive firing disappears via double limit cycle bifurcation (also known as saddle-node of limit cycles or fold of limit cycles); see Figure 1.3. Since there is a coexistence

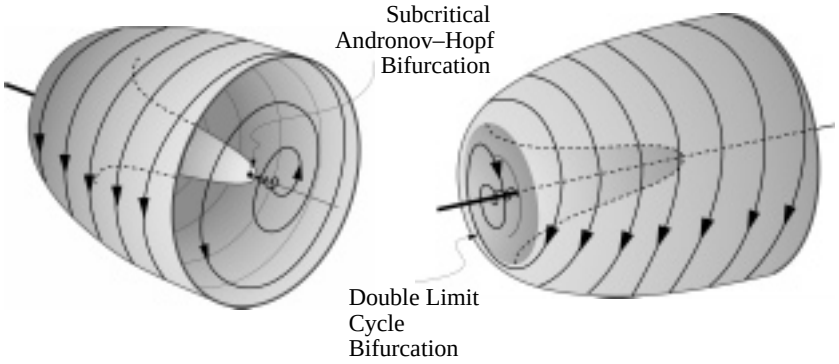

FIG. 1.3. *Subcritical elliptic burster. Rest state loses stability via subcritical Andronov–Hopf bifurcation and the limit cycle disappears via double limit cycle bifurcation (from Hoppensteadt and Izhikevich* (1997)*). Reprinted with permission from Springer-Verlag.*

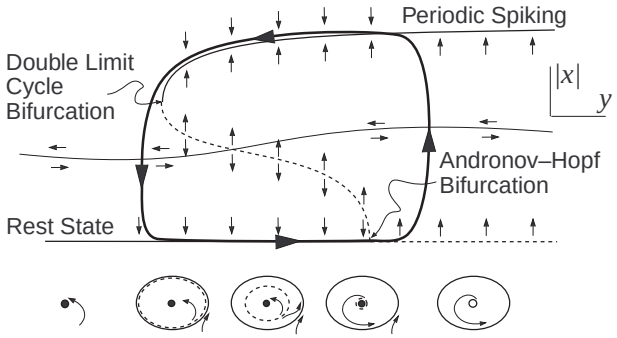

FIG. 1.4. *Subcritical elliptic burster may occur via hysteresis.*

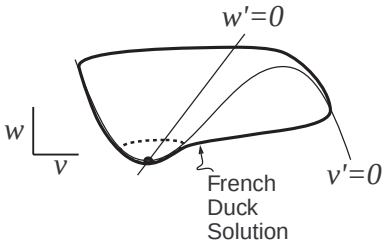

FIG. 1.5. *Nullclines, stable, and unstable limit cycles of the FitzHugh–Nagumo model.*

of rest and limit cycle attractors, the periodic transition between them often occurs via a hysteresis loop, as we illustrate in Figure 1.4. In this case the slow variable y may be one-dimensional.

1.2. Singular Hopf bifurcations and duck solutions. When the fast subsystem $\dot{x} = f(x, y)$ has many time scales, it can generate action potentials via relaxation oscillations. A typical example is the FitzHugh–Nagumo model (FitzHugh (1961))

$$\begin{aligned} \dot{v} &= v - v^3/3 - w + y, \\ \dot{w} &= \delta(a + v - bw) \end{aligned}$$

for $a = 0.7,\ b = 0.8$, and $\delta \ll 1$, whose nullclines are depicted in Figure 1.5.

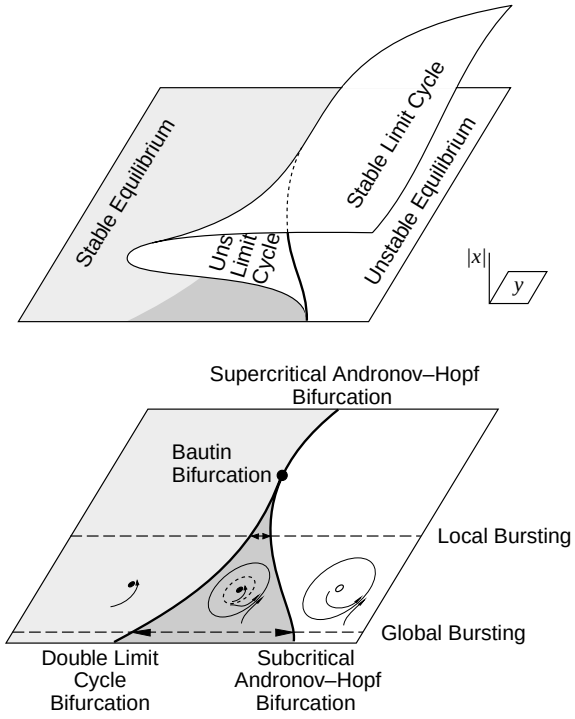

FIG. 1.6. *A neighborhood of supercritical Bautin bifurcation. Shaded area denotes the region of stability of the equilibrium corresponding to the rest state. Darker shaded area denotes the region of bistability of the equilibrium and a limit cycle attractor corresponding to the periodic firing.*

If we vary the bifurcation parameter y, the FitzHugh–Nagumo model may undergo subcritical Andronov–Hopf or double limit cycle bifurcation. A nasty problem associated with the Andronov–Hopf bifurcation in the system above is that the bifurcation is *singular* (Baer and Erneux (1986), (1992), Arnold et al. (1994)); that is, the pure imaginary eigenvalues of the Jacobian matrix at the bifurcation point have infinitesimal imaginary parts (of order $\sqrt{\delta}$). This complicates the analysis substantially, since many singular phenomena may appear, such as nonsmooth (triangular) limit cycles, French duck solutions (Eckhaus (1983)), steep growth of amplitude of oscillation, enormous disparity of interspike frequency and the frequency of small amplitude oscillations, etc.

A subcritical elliptic burster is referred to as being *singular* if the fast subsystem is of relaxation type having singular Andronov–Hopf bifurcation, and the double limit cycle bifurcation occurs in the French duck territory. A typical example of a singular subcritical elliptic burster is the FitzHugh–Rinzel model, which we consider in section 6.

1.3. Bautin bifurcation. In what follows we assume that even when the fast subsystem has many time scales, the Andronov–Hopf bifurcation is *regular* (i.e., the pure imaginary eigenvalues of the Jacobian matrix at the bifurcation point have nonvanishing imaginary parts) and the limit cycles are smooth. We refer to such subcritical elliptic bursters as being *Bautin bursters* due to the reason explained below.

Since the Andronov–Hopf and double limit cycle bifurcations have codimension 1 (Kuznetsov 1995), the corresponding bifurcation sets of the dynamical system

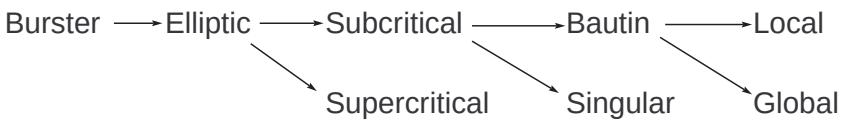

FIG. 1.7. *A partial classification of elliptic bursters.*

$\dot{x} = f(x, y)$ in the parameter space $\mathbb{R}^k \ni y$ are $k-1$ dimensional hypersurfaces. In particular, they are curves when $y \in \mathbb{R}^2$; see lower part of Figure 1.6.

Repetitive bursting occurs when slow variable y crosses the curves periodically. When the curves are far away from each other, variable y oscillates with large amplitude, and we call such Bautin burster *global*; see Figure 1.6. Quite often, however, the curves meet tangentially at a point at which a Bautin bifurcation occurs (Kuznetsov (1995)). This bifurcation, also known as degenerate or generalized Hopf bifurcation, has codimension 2, and it can be observed in many neural models, for example, in Wilson–Cowan oscillator (Borisyuk and Kirillov (1992), Hoppensteadt and Izhikevich (1997)). When the fast subsystem is near the Bautin bifurcation point so that the slow variable y has small amplitude oscillations, the burster is said to be *local*; see Figure 1.6. This is the type of elliptic bursting we study in this paper; see summary in Figure 1.7.

Any dynamical system at the Bautin bifurcation can be transformed by a suitable continuous change of variables into its topological normal form (see Kuznetsov (1995))

$$\dot{z} = (l_0 + \mathrm{i}\Omega)z + l_1 z|z|^2 + l_2 z|z|^4 \,, \tag{1.2}$$

where $z \in \mathbb{C}$ is a complex variable and Ω, l_0, l_1, and l_2 are real parameters. The last two are called first and second *Liapunov coefficients*, respectively. The Bautin bifurcation occurs when

$$l_0 = l_1 = 0 \qquad \text{but} \qquad l_2 \neq 0 \,.$$

When $l_2 < 0$ ($l_2 > 0$), the Bautin bifurcation is said to be supercritical (subcritical). From now on we consider only supercritical Bautin bifurcations.

It is easy to see that (1.2) undergoes Andronov–Hopf bifurcation for $l_0 = 0$, which is supercritical for $l_1 < 0$ and subcritical otherwise. Moreover, if $l_1 > 0$, then (1.2) undergoes double limit cycle bifurcation when

$$l_1^2 - 4 l_0 l_2 = 0; \tag{1.3}$$

see Figure 1.8. We see that both Andronov–Hopf and double limit cycle bifurcations occur simultaneously at the Bautin point $l_0 = l_1 = 0$.

The assumption that bifurcations leading to appearance and disappearance of periodic spiking in the fast system occur for nearby values of slow variable y is not new in mathematical neuroscience. It has been used successfully by Ermentrout and Kopell (1986a), (1986b) in their study of parabolic bursters. Their major achievement was derivation of canonical model for local parabolic bursters. In this paper we derive canonical model for local Bautin bursters.

1.4. Canonical model. One can easily study a model of a subcritical elliptic burster by assuming that the functions f and g in (1.1) have certain "biologically plausible" form. A potential problem is that the biological plausibility of f and g might be only an illusion. Moreover, the results predicted by the model might

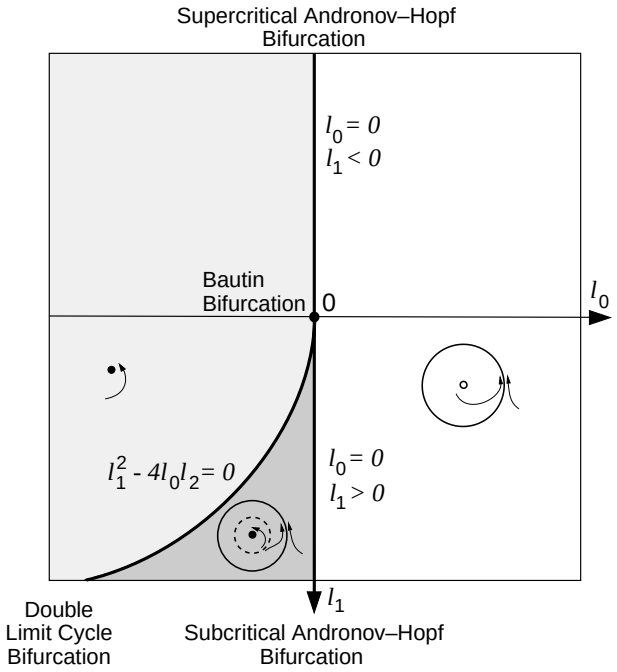

FIG. 1.8. *Supercritical Bautin bifurcation in* (1.2). *Note that the positive* l_1 *axis points downwards so that relevant regions are oriented the same way as in Figures* 1.6 *and* 2.1.

disappear when f and g are adjusted to take into account more biological data. To avoid this kind of problem Hoppensteadt and Izhikevich (1997) developed a canonical model approach, which can be summarized as follows: Instead of studying (1.1) for some f and g, let us consider all possible f and g satisfying only a few general assumptions, e.g., that the burster is local. Then we seek a continuous (possibly noninvertible) change of variables that puts (1.1) for all such f and g into a simpler model, which is called *canonical*. In section 2 we derive such a canonical model for local Bautin bursters. It has the form

$$\begin{array}{rcll} z' & = & (u + \mathrm{i}\omega)z + 2z|z|^2 - z|z|^4, & \\ u' & = & \eta(a - |z|^2), & \eta \ll 1, \end{array} \tag{1.4}$$

where $z \in \mathbb{C}$ is a new fast variable, $u \in \mathbb{R}$ is a new slow variable, and $a, \omega, \eta \in \mathbb{R}$ are parameters, and the coefficient 2 in the term $2z|z|^2$ is chosen for the sake of convenience so that the fast subsystem undergoes Andronov–Hopf and double limit cycle bifurcations for $u = 0$ and $u = -1$, respectively. We study (1.4) for $a > 0$ and $\eta \ll 1$ below.

As one expects, the fast subsystem in the canonical model (1.4) is similar to the topological normal form for Bautin bifurcation (1.2). The form of the slow subsystem might seem unexpected, since it depends neither on u nor on z or $\bar{z}$ in the first order. Detailed derivation of this equation can be found in the proof of Theorem 2.1. We just mention here that u disappears because the slow variable y oscillates with much smaller amplitude than that of x. Moreover, the frequency of x is much higher than that of y; therefore, any term that depends on the phase of x averages out, which leaves only $|z|^2$.

Finally, we notice that particulars of f and g do not affect the form of the canonical

model but affect only the values of parameters η and a. Thus, studying (1.4) for all a and η, which we do in section 3, sheds some light on dynamic behavior of all local Bautin bursters of the form (1.1) including those that have not been invented yet.

1.5. Weakly connected networks. Little is known about detailed mechanisms of bursters, much less about their networks. In this paper we assume that the bursters are weakly connected (Hoppensteadt and Izhikevich (1997)). The assumption is based on the neurophysiological observations that the average size of postsynaptic potentials (PSPs) in response to a single spike of a presynaptic cell is less than 1 mV, which is small in comparison with the average size of the action potential (around 100 mV). For example, PSPs in hippocampus cells are as small as 0.1 ± 0.03 mV (McNaughton et al. (1981), Sayer, Friedlander, and Redman (1990)). The majority of PSPs in pyramidal neurons of the rat visual cortex are less than 0.5 mV, with the range $0.05 - 2.08$ mV (Mason, Nicoll, and Stratford (1991)). As was pointed out by Mason, Nicoll, and Stratford (1991), there is an underestimate of the true range because PSPs smaller than 0.03 mV would usually not be detected.

Weakly connected networks of bursters can be written in the "weakly connected" form

$$\begin{aligned} \dot{x}_i &= f_i(x_i, y_i) + \epsilon p_i(x, y, \varepsilon), \\ \dot{y}_i &= \mu\{g_i(x_i, y_i) + \epsilon q_i(x, y, \varepsilon)\}, \end{aligned} \tag{1.5}$$

where each pair $(x_i, y_i) \in \mathbb{R}^m \times \mathbb{R}^k$ describes the activity of the ith burster, the functions p_i and q_i define how the bursters interact, and the parameter $\epsilon \in \mathbb{R}$ is small reflecting the strength of connections in the network. Hoppensteadt and Izhikevich (1997) obtained the estimate

$$0.004 < \epsilon < 0.008$$

using experimental data from the hippocampus (McNaughton, Barnes, and Andersen (1981)).

It is a daunting task to study (1.5) without even knowing how p_i and q_i look. We use the assumption $\epsilon \ll 1$ to achieve this goal. In section 4 we show that (1.5), satisfying a few additional assumptions, can be transformed into the canonical model

$$\begin{aligned} z_i' &= (b_i u_i + \mathrm{i}\omega_i) z_i + c_i z_i |z_i|^2 - d_i z_i |z_i|^4 + \sum_{j=1}^{n} c_{ij} z_j, \\ u_i' &= \eta_i (a_i - |z_i|^2) \end{aligned}$$

by a suitable change of variables. Here $z_i \in \mathbb{C}$ and $u_i \in \mathbb{R}$ are new fast and slow variables, respectively, and $a_i, \omega_i, \eta_i \in \mathbb{R}$, $b_i, c_i, d_i, c_{ij} \in \mathbb{C}$ are parameters that depend on particulars of the functions f_i, g_i, p_i, and q_i. We analyze the canonical model above in section 5, then we compare its behavior with that of a network of FitzHugh–Rinzel bursters in section 6, and discuss our findings in section 7.

2. Derivation of the canonical model. Consider a singularly perturbed dynamical system of the form

$$\begin{aligned} \dot{x} &= f(x, y), \\ \dot{y} &= \mu g(x, y), \end{aligned} \tag{2.1}$$

where $x \in \mathbb{R}^m$, $y \in \mathbb{R}^k$, $\mu \ll 1$, and the functions f and g are sufficiently smooth. We say that this system describes a *Bautin burster* if the following conditions are satisfied.

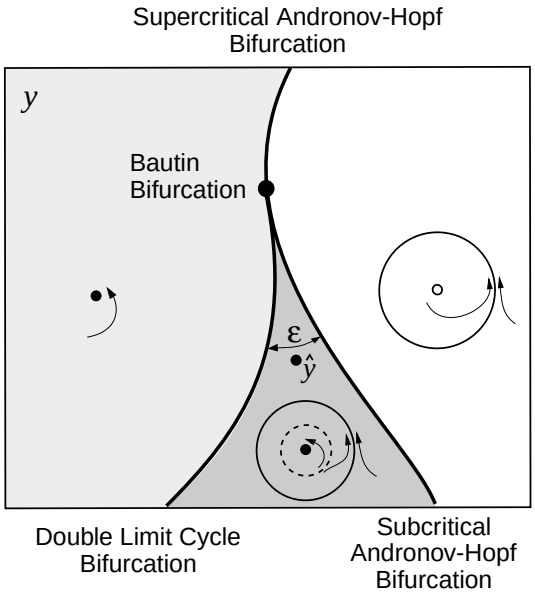

FIG. 2.1. *System* (2.1) *is a local subcritical elliptic burster when the fast subsystem is near Bautin bifurcation and the slow subsystem has a stable equilibrium* $\hat{y}$ *in the shaded area where attractors coexist.*

C1. Fast subsystem $\dot{x} = f(x, y)$ undergoes supercritical Bautin (generalized Hopf) bifurcation at $x = 0$ for $y = 0$, where $y \in \mathbb{R}^k$ is treated as a vector of bifurcation parameters.

C2. Slow subsystem $\dot{y} = \mu g(0, y)$ has an exponentially stable equilibrium $\hat{y}$ in the area where the rest and limit cycle attractor of the fast subsystem coexist; see Figure 2.1.

The Bautin burster is said to be *local* if $\hat{y}$ is near the Bautin bifurcation point $y = 0$. Let $\varepsilon \ll 1$ be proportional to the distance between the subcritical Andronov–Hopf bifurcation and the double limit cycle bifurcation near the equilibrium $\hat{y}$, as in Figure 2.1. We require $\varepsilon \gg \mu^{4/3}$ so that we may use averaging in the proof of the theorem below.

THEOREM 2.1 (Canonical model for local Bautin bursters). *There is a continuous change of variables that transforms all local Bautin bursters* (2.1) *into the canonical model*

$$\begin{array}{rcl} z' & = & (u + \mathrm{i}\omega)z + 2z|z|^2 - z|z|^4 \\ u' & = & \eta(a \pm |z|^2) \end{array} \quad + \ \mathcal{O}(\sqrt[4]{\varepsilon}) \,, \tag{2.2}$$

where $' = d/d\tau$, $\tau = \mathcal{O}(\varepsilon)t$ *is slow time,* $z \in \mathbb{C}$, *and* $u \in \mathbb{R}$ *are new fast and slow variables, respectively, and* $a, \omega \in \mathbb{R}$ *and* $\eta = \mathcal{O}(\mu/\varepsilon^{3/2})$ *are parameters.*

Nonzero values of $z(\tau)$ correspond to periodic spiking of the fast variable $x(t)$ with the amplitude of order $\sqrt[4]{\varepsilon}|z|$ and the interspike frequency of order Ω (see Figure 2.2), where $\pm\mathrm{i}\Omega$ are the pure imaginary eigenvalues of the fast subsystem $\dot{x} = f(x, y)$ at the Bautin point $(x, y) = (0, 0)$. The canonical model exhibits bursting when $0 < a < 1$ and tonic spiking when $a > 1$.

The canonical model (2.2) loses its significance when $a < 0$ or there is a term $+|z|^2$ since the slow variable u leaves any finite neighborhood of the origin and approaches

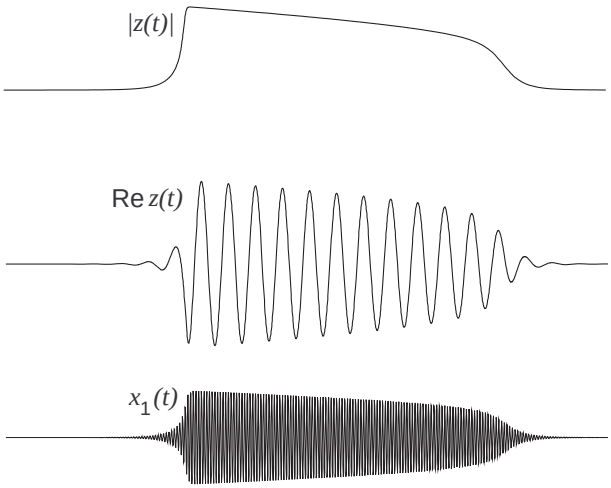

FIG. 2.2. *The relationship between* $z \in \mathbb{C}$ *and* $x \in \mathbb{R}^m$ (*simulation parameters:* $a = 0.8,\ \eta = \varepsilon = 0.1,\ \Omega = \omega = 3,\ t \in [0, 500]$).

$\pm\infty$ for almost all initial conditions. This corresponds to slow variable y leaving a small neighborhood of the Bautin point where the theorem is applicable.

Proof. The proof is a standard application of center manifold reduction and Poincaré normal form transformation to (2.1); see the book by Hoppensteadt and Izhikevich (1997). We outline it briefly below.

Center manifold reduction. Consider system (2.1) in a neighborhood of the point $(x, y) = (0, 0)$ for $\mu = 0$. It has a local $(2 + k)$-dimensional center manifold M tangent to the subspace $E^{\mathrm{c}} \times \mathbb{R}^k$, where E^{c} is spanned by the eigenvectors of the Jacobian matrix $J = D_x f(0, 0)$ corresponding to purely imaginary eigenvalues $\pm\mathrm{i}\Omega$. The manifold is invariant, and there is a continuous transformation $h_M : \mathbb{R}^m \times \mathbb{R}^k \times \mathbb{R} \to M$ that maps local solutions of (2.1) into those of the (restricted) system

$$\begin{aligned} \dot{\tilde{x}} &= f(\tilde{x}, \tilde{y}), \\ \dot{\tilde{y}} &= \mu g(\tilde{x}, \tilde{y}), \end{aligned} \tag{2.3}$$

where $(\tilde{x}, \tilde{y}) = h_M(x, y, \mu) \in M$. Since we will use the initial portion of Taylor expansions of f and g below, we are not concerned with the nonuniqueness of the center manifold; see discussion by Guckenheimer and Holmes (1983).

Now the fast subsystem is two-dimensional. It undergoes Bautin bifurcation at $\tilde{x} = 0$ for $\tilde{y} = 0$. Since the 2×2 Jacobian matrix at the Bautin point has complex conjugate eigenvalues $\pm\mathrm{i}\Omega$, it is nonsingular, and from the implicit function theorem it follows that the fast subsystem has a family of equilibria parametrized by $\tilde{y}$.

Poincaré normal form transformation. There is a mapping $h_P : M \to \mathbb{C}$ that transforms the fast subsystem $\dot{\tilde{x}} = f(\tilde{x}, \tilde{y})$ into its Poincaré normal form

$$\dot{w} = L_0(\tilde{y})w + L_1(\tilde{y})w|w|^2 + L_2(\tilde{y})w|w|^4 + \mathcal{O}(w^7)\ , \tag{2.4}$$

where $w = h_P(\tilde{x}, \tilde{y}) \in \mathbb{C}$, and the function L_0 denotes the perturbation of the eigenvalue $\mathrm{i}\Omega$ for small $\tilde{y}$. Introduction of a new time $\tilde{t}$ such that

$$dt = \{1 - (\operatorname{Im} L_0 + \operatorname{Im} L_1|w|^2)/\Omega \ + \ (\operatorname{Im} L_2/\Omega - (\operatorname{Im} L_1)^2/\Omega^2)|w|^4\}d\tilde{t} \tag{2.5}$$

transforms the normal form into

$$\dot{w} = (l_0(\tilde{y}) + \mathrm{i}\Omega)w + l_1(\tilde{y})w|w|^2 + l_2(\tilde{y})w|w|^4 + \mathcal{O}(w^7)\ , \tag{2.6}$$

where $l_0,\ l_1$, and l_2 are real-valued functions such that

$$l_0(0) = l_1(0) = 0 \qquad \text{but} \qquad l_2(0) < 0\ .$$

That is, $\tilde{y} = 0$ is the supercritical Bautin bifurcation point for (2.6).

Blowing up of the fast subsystem. Since the equilibrium $\hat{y}$ of the slow subsystem is near the Bautin bifurcation point, both $|l_0(\hat{y})|$ and $|l_1(\hat{y})|$ are small. Let

$$\varepsilon = \frac{l_1^2(\hat{y})}{4|l_2(0)|} \tag{2.7}$$

be a small parameter, which has the same order of magnitude as the distance between Andronov–Hopf bifurcation and double limit cycle bifurcation; see Figure 2.1. The change of variables

$$w = \frac{\sqrt[4]{\varepsilon}}{\sqrt[4]{|l_2(0)|}}\, e^{\mathrm{i}\Omega t} z\ , \tag{2.8}$$

$$l_0(\tilde{y}) = \varepsilon v \tag{2.9}$$

transforms (2.6) into

$$\dot{z} = \varepsilon\{vz + 2z|z|^2 - z|z|^4\ +\ \mathcal{O}(\sqrt{\varepsilon})\}\ , \tag{2.10}$$

where we used

$$\begin{aligned} \tilde{y} &= \hat{y} + \mathcal{O}(\varepsilon)\ , \\ l_1(\tilde{y}) &= l_1(\hat{y}) + \mathcal{O}(\varepsilon)\ , \\ l_2(\tilde{y}) &= l_2(0) + \mathcal{O}(\sqrt{\varepsilon})\ . \end{aligned} \tag{2.11}$$

Averaging of the slow subsystem. Notice that the new slow variable, v, is a scalar even though y is a k-dimensional vector. Differentiating (2.9) with respect to t yields $\varepsilon\dot{v} = D_y l_0(\tilde{y})\,\dot{\tilde{y}}$. Since g is sufficiently smooth, the initial portion of the Taylor series of the slow subsystem exists and may be rewritten in new variables in the form

$$\dot{v} = \frac{\mu}{\varepsilon^{3/4}}\alpha_1 \operatorname{Re} e^{\mathrm{i}\Omega t} z\ +\ \frac{\mu}{\varepsilon^{1/2}}\left(\alpha_2 + \alpha_3 \operatorname{Re} e^{2\mathrm{i}\Omega t} z^2 + \alpha_4|z|^2\right)\ +\ \mathcal{O}\left(\frac{\mu}{\varepsilon^{1/4}}\right)\ . \tag{2.12}$$

Since $\mu/\varepsilon^{3/4}$ is small, we use the near identity transformation

$$v(t) = u(t) + \frac{\mu}{\varepsilon^{3/4}}\int_0^t \alpha_1 \operatorname{Re} e^{\mathrm{i}\Omega s} z\, ds + \frac{\mu}{\varepsilon^{1/2}}\int_0^t \alpha_3 \operatorname{Re} e^{2\mathrm{i}\Omega s} z^2\, ds, \tag{2.13}$$

which is equivalent to averaging, to transform the slow subsystem to

$$\dot{u} = \frac{\mu}{\sqrt{\varepsilon}}(\alpha_2 + \alpha_4|z|^2\ +\ \mathcal{O}(\sqrt[4]{\varepsilon})). \tag{2.14}$$

The equations (2.10) and (2.14) can be written in the canonical form (2.2), where $\tau = \varepsilon\tilde{t}$ is slow time, $\eta = \mu|\alpha_4|/\varepsilon^{3/2}$ and $a = \alpha_2/|\alpha_4|$.

Since the canonical model is invariant under the rotation $z \to z\varepsilon^{\mathrm{i}\varphi}$, we may introduce an arbitrary (dummy) parameter ω, which defines the frequency of oscillation of the canonical variable z in slow time τ.

Finally, the transformation $h : \mathbb{R}^m \times \mathbb{R}^k \times \mathbb{R} \to \mathbb{C} \times \mathbb{R}$ that maps solutions of the local Bautin burster (2.1) to those of the canonical model (2.2) is the superposition of transformations h_M, h_P, rescaling (2.8), projection (2.9), and averaging (2.13). ∎

When we consider behavior of the canonical model on a large time scale of order $1/\eta$, small terms hidden in $\mathcal{O}(\sqrt[4]{\varepsilon})$ might become large and hence cannot be neglected. To avoid this we require that $\sqrt[4]{\varepsilon}/\eta \ll 1$, which is equivalent to the requirement that $\varepsilon^{7/4} \ll \mu$. Thus, if the distance between the bifurcations, ε, satisfies

$$\mu^{4/3} \ll \varepsilon \ll \mu^{4/7}\,, \tag{2.15}$$

then we may neglect the $\mathcal{O}(\sqrt[4]{\varepsilon})$ terms in the canonical model (2.2) when we study it on the time scale of order $1/\eta$. Finally, notice that if $\varepsilon = \mathcal{O}(\mu^{2/3})$, then $\eta = \mathcal{O}(1)$ might not be small. Thus, the canonical model (2.2) may not be singularly perturbed even though the original system (2.1) is.

Remark 2.2. The slow variable u does not participate in the second equation in the canonical model (2.2). Indeed, from (2.11), it follows that deviations of y from the constant $\hat{y}$ have small order and affect only the $\mathcal{O}$ term in (2.12), (2.14), and hence in (2.2). Therefore, qualitative and quantitative changes that are due to the projection of a multidimensional slow variable $y \in \mathbb{R}^k$ onto a single scalar u can reveal themselves only on the time scale of order larger than $1/\eta$.

3. Analysis of the canonical model. It is easy to see that the choice $+|z|^2$ in the canonical model (2.2) cannot produce periodic bursting behavior, since the slow variable u leaves any finite neighborhood of the origin and approaches $\pm\infty$ depending on the value of a and the initial condition. Below we consider the choice $-|z|^2$. Let $r = |z|$ denote the amplitude of oscillation of the fast variable $z \in \mathbb{C}$. We neglect the term $\mathcal{O}(\sqrt[4]{\varepsilon})$ and rewrite the canonical model (2.2) in the form

$$\begin{aligned} r' &= ur + 2r^3 - r^5, \\ u' &= \eta(a - r^2). \end{aligned} \tag{3.1}$$

Nontrivial ($r \neq 0$) equilibria of this system correspond to limit cycles of the canonical model (2.2), which may look like periodic (tonic) spiking with frequency ω. Limit cycles of this system correspond to periodic or quasi-periodic solutions of (2.2), which look like bursting; see Figure 3.1.

System (3.1) has a unique equilibrium

$$\begin{pmatrix} r \\ u \end{pmatrix} = \begin{pmatrix} \sqrt{a} \\ a^2 - 2a \end{pmatrix}$$

for all η and $a > 0$, which is stable when $a > 1$. When a decreases and passes an η-neighborhood of $a = 1$, the equilibrium loses stability via quasi-static saddle-node bifurcation (Hoppensteadt and Izhikevich (1997)), which is also referred to as singular Hopf bifurcation (Baer and Erneux (1986), (1992), Arnold et al. (1994)). Among many interesting features of this bifurcation is the existence of French ducks (canards); see Eckhaus (1983) and the middle part of Figure 3.1. When $0 < a < 1$, the system (3.1) has a limit cycle attractor. Therefore, the canonical model (2.2) and the original system (2.1) exhibit bursting behavior; see upper part of Figure 3.1. The

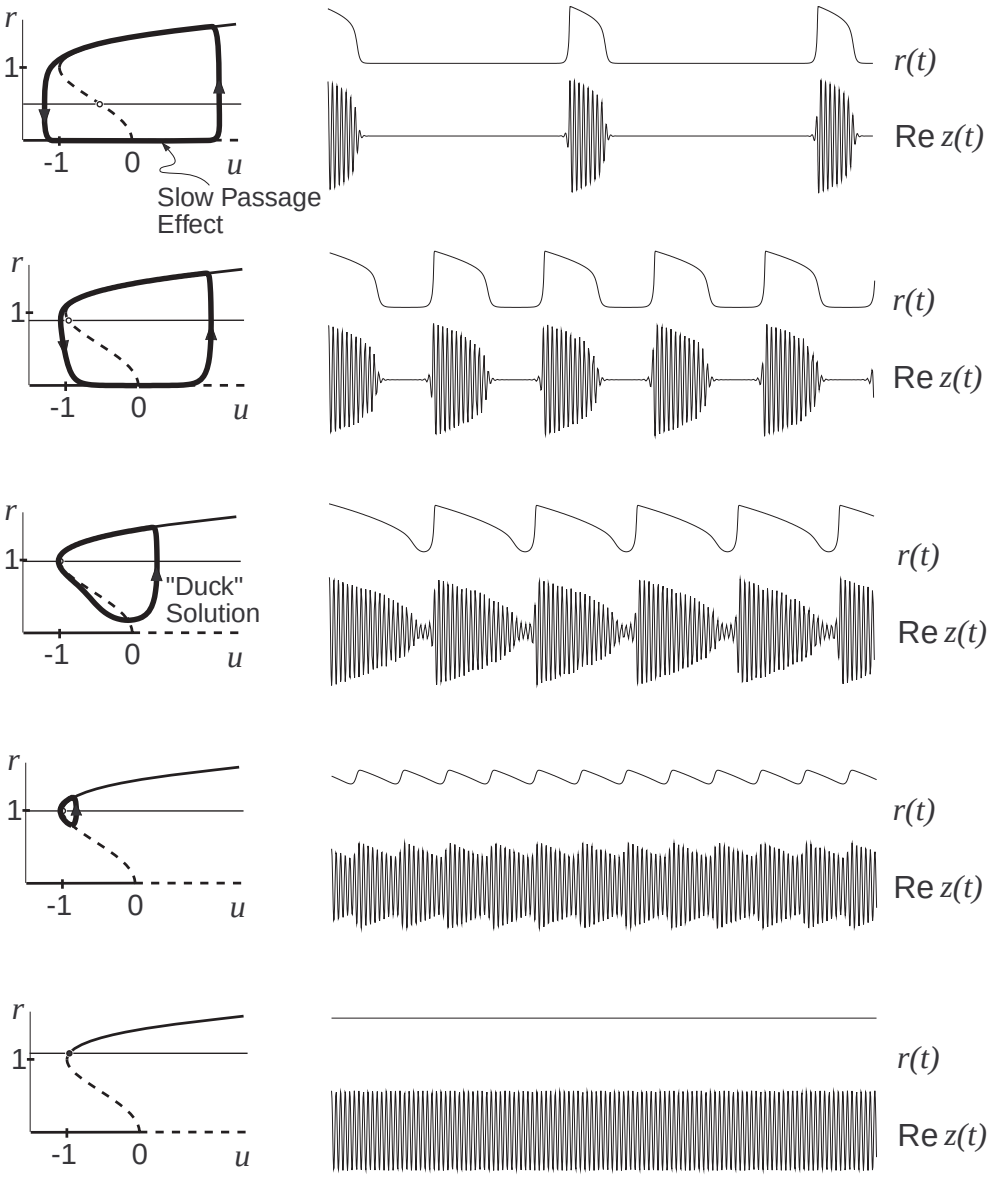

FIG. 3.1. *Phase portrait and solution of the canonical model* (3.1) *for* $\eta = 0.1$, $\omega = 3$ *and various* a. *From top to bottom:* $a = 0.25$, $a = 0.8$, $a = 0.986$, $a = 0.987$, *and* $a = 1.2$.

smaller a is, the longer is the interburst period. When $a \to 0$, the interburst period becomes infinite.

Notice that the system (3.1) cannot be used to analyze completely behavior of the canonical model (2.2) for $a \approx 1$ and/or $a \approx 0$ since small terms hidden in $\mathcal{O}(\sqrt[4]{\varepsilon})$ might not be negligible in this case.

3.1. Slow passage effect. The equilibrium $r = 0$ of the fast subsystem is stable if and only if $u < 0$. One might expect that the fast variable r jumps to the upper branch as soon as u becomes positive. This is not the case when u passes

the bifurcation value $u = 0$ slowly. Fast variable r continues to be small even for positive u due to the slow passage effect (see Nejshtadt (1985), Baer, Erneux, and Rinzel (1989), Holden and Erneux (1993a,b), and Arnold et al. (1994)), which is also referred to as being memory or ramp effect. It can be observed even for intermediate η. For example, we use $\eta = 0.1$ in Figure 3.1.

Suppose there is no noise or any influences from other bursters. When $u < 0$, the fast variable r spends $1/(\eta a)$ units of time approaching the origin. When u crosses the bifurcation value $u = 0$, the equilibrium $r = 0$ becomes unstable, but r is so near the equilibrium that it might take a sizable period of time to diverge from it.

The slow passage effect is very sensitive to whether or not the system is analytical (Nejshtadt (1985)). For example, the canonical model (3.1) is analytical; therefore, the effect is noticeable, i.e., it occurs for $u = \mathcal{O}(1)$. In contrast, we do not assume that the original system (2.1) is analytical; therefore, the slow passage effect there may be negligible, i.e., it occurs for $y = o(1)$. These two observations do not contradict each other because u describes dynamics of y in a blown-up neighborhood of the Bautin bifurcation point; that is, $\mathcal{O}(1)$-amplitude oscillation of u corresponds to $\mathcal{O}(\varepsilon)$-amplitude oscillation of y, as it follows from (2.9) and (2.13) or from Figure 2.1.

The slow passage effect can be shortened significantly by noise or weak input from other bursters. We discuss the former below and the latter in section 4.

3.2. Noise. Instead of using stochastic differential equations to study the effect of noise, we assume that the bursters can be written in the form

$$\begin{aligned} \dot{x} &= f(x, y, \varepsilon I(t)), \\ \dot{y} &= \mu g(x, y, \varepsilon I(t)), \end{aligned} \tag{3.2}$$

where $I(t)$ is a multidimensional noisy signal, e.g., that from other bursters or external receptors, and $\varepsilon \ll 1$ is defined in (2.7); see also Figure 2.1.

THEOREM 3.1 (canonical model for local Bautin bursters with noise). *There is a continuous time dependent change of variables that transforms all local Bautin bursters of the form* (3.2) *into the canonical model*

$$\begin{aligned} z' &= b + uz + 2z|z|^2 - z|z|^4, \\ u' &= \eta(a \pm |z|^2) \end{aligned} \tag{3.3}$$

plus high-order terms, where $b \in \mathbb{C}$ *is a linear function of*

$$\lim_{T\to\infty} \frac{1}{T} \int_0^T e^{-\mathrm{i}\Omega t} I(t)\, dt \tag{3.4}$$

provided that the limit exists.

Proof. Proceeding as in the proof of Theorem 2.1, we obtain the truncated normal form

$$\dot{w} = \varepsilon N(t) + (l_0 + \mathrm{i}\Omega)w + l_1 w|w|^2 + \ l_2 w|w|^4,$$

which is an analogue of (2.6). Here N is a function of I, and we disregarded terms of order w^7 and ε^2. The transformations (2.8) and (2.9) transform the equation above into

$$\dot{z} = \varepsilon\{e^{-\mathrm{i}\Omega t} N(t) + vz + 2z|z|^2 - z|z|^4\}\ , \tag{3.5}$$

where we incorporated the constant $\sqrt[4]{2|l_2|}$ into $N(t)$. Let

$$b = \lim_{T\to\infty} \frac{1}{T} \int_0^T e^{-\mathrm{i}\Omega t} N(t)\, dt$$

denote the average of $e^{-\mathrm{i}\Omega t}N(t)$. The nearly identity change of variables, which is equivalent to averaging,

$$z = w + \varepsilon \int_0^t (e^{-\mathrm{i}\Omega s} N(s) - b)\, ds \tag{3.6}$$

transforms (3.5) into

$$\dot{w} = \varepsilon\{b + vw + 2w|w|^2 - w|w|^4\}$$

plus terms of higher order. After we average the slow subsystem and introduce the slow time $\tau = \varepsilon t$, we obtain the canonical model of the form (3.3). □

A word of caution is in order. The averaging given by the change of variables (3.6) is accurate on the time scale of order $1/\varepsilon$ (original time t) unless additional assumptions are imposed. Therefore, the canonical model (3.3) may not be accurate on a time scale of order greater than 1 (slow time $\tau = \varepsilon t$). That is, the higher order terms that we neglected in (3.3) may become significant on the large time scale.

Notice that $b = 0$ when the quantity defined in (3.4) vanishes. We say that the input $I(t)$ is nonresonant in this case. Thus, we have the following observation.

Remark 3.2 (Baer, Erneux, and Rinzel (1989)). The slow passage effect is not affected by noisy signal $I(t)$ unless $I(t)$ is resonant; i.e., it has frequency Ω in its power spectrum.

Suppose $I(t)$ denotes a weak input from other bursters; then the input is functionally insignificant unless it is resonant with the frequency Ω. We return to this issue in Corollary 4.2 below and in the discussion section.

Let us rewrite the canonical model (3.3) with the choice $-|z|^2$ in polar coordinates $w = re^{\mathrm{i}\varphi}$:

$$\begin{aligned} r' &= \operatorname{Re} e^{-\mathrm{i}\varphi} b + ur + 2r^3 - r^5, \\ \varphi' &= \tfrac{1}{r} \operatorname{Im} e^{-\mathrm{i}\varphi} b, \\ u' &= \eta(a - r^2). \end{aligned}$$

Let $b = |b|e^{\mathrm{i}\beta} \neq 0$; then the middle equation can be written in the form

$$\varphi' = \frac{|b|}{r} \sin(\beta - \varphi)$$

from which we conclude that $\varphi \to \beta$. Therefore, $\operatorname{Re} e^{-\mathrm{i}\varphi} b \to |b|$, and we obtain the system

$$\begin{aligned} r' &= |b| + ur + 2r^3 - r^5, \\ u' &= \eta(a - r^2). \end{aligned} \tag{3.7}$$

Nullclines of the fast subsystem for $b = 0$ and $b \neq 0$ are depicted in Figure 3.2.

Since r is always nonnegative, we use the upper parts of the nullclines in Figure 3.1 ($b = 0$) and in Figure 3.3 ($b = 0.05$). The latter shows that the slow passage effect disappears, and the burster behaves as a relaxation oscillator of Bonhoeffer–Van der Pol type.

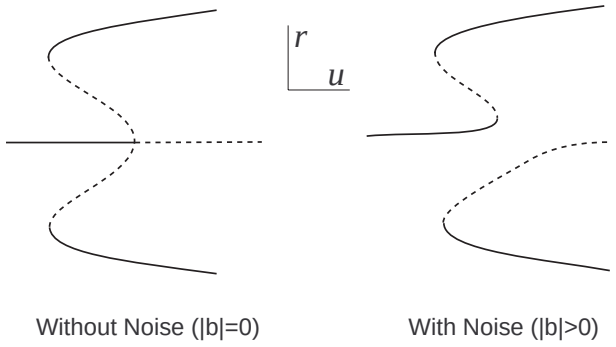

FIG. 3.2. *Nullclines of the fast subsystem* $r' = |b| + ur + 2r^3 - r^5$ *for* $b = 0$ *(left) and* $b = 0.05$ *(right).*

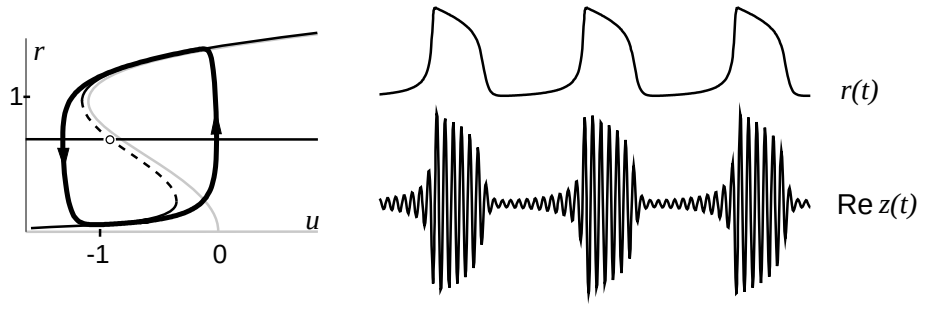

FIG. 3.3. *Solution of* (3.7) *for* $b = 0.05,\ \eta = 0.1,\ a = 0.5$ *(nullclines for* $b = 0$ *are depicted as light curves for comparison).*

4. Weakly connected bursters. Consider a weakly connected system of the form

$$\begin{aligned} \dot{x}_i &= f_i(x_i, y_i) + \epsilon p_i(x, y, \epsilon), \\ \dot{y}_i &= \mu_i\{g_i(x_i, y_i) + \epsilon q_i(x, y, \epsilon)\}, \end{aligned} \tag{4.1}$$

and suppose that each equation in the uncoupled network

$$\begin{aligned} \dot{x}_i &= f_i(x_i, y_i), \\ \dot{y}_i &= \mu_i g_i(x_i, y_i), \end{aligned} \qquad i = 1, \ldots, n\ , \tag{4.2}$$

is a local Bautin burster; see conditions C1 and C2 above. Notice that we have many small parameters: the strength of connections ϵ, the distance between Andronov–Hopf and double limit cycle bifurcations ε, and the slow time scales $\mu_i,\ \ i = 1, \ldots, n$. We require that each μ_i satisfy (2.15) so that we may use averaging in the theorem below. We also assume that $\epsilon = \mathcal{O}(\varepsilon)$, which incidentally does not exclude the case $\epsilon = o(\varepsilon)$. Without loss of generality we may set $\epsilon = \varepsilon$ and incorporate the $\mathcal{O}(1)$ factor into the connection functions p_i and q_i.

Proceeding as in the proof of Theorem 2.1 above, we apply center manifold reduction and Poincaré normal form transformation to each fast subsystem $\dot{x}_i = f_i(x_i, y_i)$ to obtain its normal form

$$\dot{w}_i = L_{0i}(y_i)w_i + L_{1i}(y_i)w_i|w_i|^2 + L_{2i}(y_i)w_i|w_i|^4 + \mathcal{O}(w_i^7)\ , \tag{4.3}$$

which is similar to (2.4). When $n = 1$, we used new time $\tilde{t}$ defined in (2.5) to remove $\operatorname{Im} L_{0i}$, $\operatorname{Im} L_{1i}$, and $\operatorname{Im} L_{2i}$ from the normal form. We cannot use such $\tilde{t}$ when $n > 1$, which complicates analysis substantially.

Recall that the parameter $\operatorname{Im} L_{0i} = \Omega_i > 0$ is the natural interspike frequency of the ith burster. The actual interspike frequency depends on the amplitude of oscillations. If $|w_i| = \mathcal{O}(\sqrt[4]{\varepsilon})$, then the frequency is

$$\Omega_i + \Lambda_i |w_i|^2 + \mathcal{O}(\varepsilon),$$

where $\Lambda_i = \operatorname{Im} L_{1i}(0)$. For the sake of simplicity we assume that the following conditions are satisfied for all i.

C3. The interspike frequency does not depend (up to order $\mathcal{O}(\varepsilon)$) on the amplitude of spiking; that is, $\operatorname{Im} L_{1i}(0) = 0$.

C4. The slow variable y_i is a scalar.

We discuss the general case later.

THEOREM 4.1 (canonical model for weakly connected local Bautin bursters). *Consider a network of weakly connected local Bautin bursters* (4.1) *satisfying conditions* C3 *and* C4 *above. There is an* $\varepsilon_0 > 0$ *such that for all* $\varepsilon \le \varepsilon_0$ *there is a continuous change of variables that transforms the network into the canonical model*

$$\begin{array}{rcl} z_i' &=& (b_i u_i + \mathrm{i}\omega_i) z_i + c_i z_i |z_i|^2 - d_i z_i |z_i|^4 + \sum_{j=1}^n c_{ij} z_j \\ u_i' &=& \eta_i (a_i \pm |z_i|^2) \end{array} + \mathcal{O}(\sqrt[4]{\varepsilon}), \tag{4.4}$$

where $' = d/d\tau$, $\tau = \varepsilon t$ *is slow time, and* $z_i \in \mathbb{C}$ *and* $u_i \in \mathbb{R}$ *are new fast and slow variables describing the* i*th burster, respectively. Parameters* $\omega_i \in \mathbb{R}$ *are center interspike frequencies, which denote* ε*-deviations from the natural interspike frequencies* Ω_i, $\eta_i = \mathcal{O}(\mu_i/\varepsilon^{3/2})$, $a_i \in \mathbb{R}$, $b_i, c_i, d_i \in \mathbb{C}$ *are parameters,* $i = 1, \dots, n$. *The synaptic coefficient* $c_{ij} \in \mathbb{C}$ *vanishes when the* i*th and the* j*th bursters have different natural interspike frequencies* Ω_i.

COROLLARY 4.2. *Local Bautin bursters do not interact unless they have matching interspike frequencies* Ω_i.

Thus, in order to establish communication, it is not enough to grow synaptic connections between such bursters; they must also establish common interspike frequency. This mechanism resembles selective tuning in radio, and it seems to be a general principle of communication between weakly connected periodically spiking neurons (Hoppensteadt and Izhikevich (1996a), (1997), (1998)). Notice though that distinct *interburst* frequencies do not prevent the communication.

The corollary needs some adjustment when the interspike frequency depends essentially on the amplitude of spiking. We discuss this issue in section 6.3.

Remark 4.3. Even though we do not make any assumptions about the connection functions p_i and q_i in the weakly connected system (4.1), the connections between bursters in the canonical model (4.4) become linear, where c_{ij} depend on the partial derivatives $D_{x_j} p_i$ at the Bautin bifurcation point. This is the consequence of the fact that each x_j oscillates with a small amplitude, therefore only linear terms are relevant up to the leading order.

Remark 4.4. It is not correct to assume that positive (negative) c_{ij} implies immediately that the synaptic connection between the corresponding bursters is excitatory (inhibitory). Each complex coefficient $c_{ij} = s_{ij} e^{\mathrm{i}\psi_{ij}}$ describes the amplitude and polarity of the connection, where $s_{ij} = |c_{ij}|$ gives the rescaled synaptic strength, and $\psi_{ij} = \operatorname{Arg} c_{ij}$ encodes phase information about the synaptic connection, which we call the *natural phase difference* (Hoppensteadt and Izhikevich (1996a), (1997)). There we

show that the relationship between c_{ij} and the sign of synaptic connection is subtler than one might think.

Proof. The proof is similar to that of Theorem 2.1. First, we use center manifold reduction for weakly connected systems (Hoppensteadt and Izhikevich (1997)) to reduce (4.1) onto its center manifold. Such transformation exists for all ε smaller than certain $\varepsilon_0 > 0$ (Fenichel (1971)). Then we apply Poincaré normal form transformation to each fast subsystem to obtain its Poincaré normal form (4.3). Since each equation in (4.2) describes a local Bautin burster, we have

$$\begin{aligned} y_i &= \mathcal{O}(\sqrt{\varepsilon}) \,, \\ \operatorname{Re} L_{0i} &= \mathcal{O}(\varepsilon) \,, \\ \operatorname{Re} L_{1i} &= \mathcal{O}(\sqrt{\varepsilon}) \,. \end{aligned}$$

The initial portion of Taylor series of each L for $y_i = \mathcal{O}(\sqrt{\varepsilon})$ can be written in the form

$$\begin{aligned} L_{0i}(y) &= \mathrm{i}\Omega_i + \sqrt{\varepsilon}\mathrm{i}\Delta_i + \varepsilon(b_i u_i + \mathrm{i}\omega_i) + \mathcal{O}(\varepsilon\sqrt{\varepsilon}), \\ L_{1i}(y) &= \sqrt{\varepsilon}c_i + \mathcal{O}(\varepsilon) \,, \\ L_{2i}(y) &= -d_i + \mathcal{O}(\sqrt{\varepsilon}) \,, \end{aligned}$$

where $\Omega_i + \sqrt{\varepsilon}\Delta_i$ is the natural interspike frequency of the ith burster, $\omega_i \in \mathbb{R}$ is the frequency deviation, and $b_i, c_i, d_i \in \mathbb{C}$ are some parameters satisfying $\operatorname{Re} c_i > 0$ and $\operatorname{Re} d_i > 0$. Notice that the Taylor series of $L_{1i}(y)$ starts from the $\sqrt{\varepsilon}$ term due to the condition C3, and that each variable u_i is one-dimensional due to the condition C4.

Application of the Poincaré transformation to the weakly connected fast subsystems

$$\dot{x}_i = f_i(x_i, y_i) + \varepsilon p_i(x, y, \varepsilon)$$

results in

$$\begin{aligned} \dot{w}_i = {} & (\mathrm{i}\Omega_i + \sqrt{\varepsilon}\mathrm{i}\Delta_i + \varepsilon(b_i u_i + \mathrm{i}\omega_i))w_i + \sqrt{\varepsilon}c_i w_i |w_i|^2 - d_i w_i |w_i|^4 \\ & + \varepsilon \left(p_i + \sum_{j=1}^{n} (c_{ij} w_j + e_{ij} \bar{w}_j) \right) + \text{h.o.t.} \,, \end{aligned}$$

where p_i, c_{ij} and e_{ij} are some complex-valued coefficients, and h.o.t. denotes higher-order terms. The change of variables

$$w_i = \sqrt[4]{\varepsilon} e^{\mathrm{i}(\Omega_i + \sqrt{\varepsilon}\Delta_i)t} \tilde{z}_i + \varepsilon \mathrm{i} p_i / \Omega_i$$

transforms the system above into

$$\begin{aligned} \varepsilon^{-1} \dot{\tilde{z}}_i = {} & (b_i u_i + \mathrm{i}\omega_i)\tilde{z}_i + c_i \tilde{z}_i |\tilde{z}_i|^2 - d_i \tilde{z}_i |\tilde{z}_i|^4 \\ & + \sum_{j=1}^{n} c_{ij} e^{\mathrm{i}(\Omega_j - \Omega_i + \sqrt{\varepsilon}(\Delta_j - \Delta_i))t} \tilde{z}_j \\ & + \sum_{j=1}^{n} e_{ij} e^{-\mathrm{i}(\Omega_j + \Omega_i + \sqrt{\varepsilon}(\Delta_j + \Delta_i))t} \bar{\tilde{z}}_j \\ & + \mathcal{O}(\sqrt[4]{\varepsilon}). \end{aligned}$$

We can use averaging to remove all terms having $e^{\mathrm{i}\delta t}$ for $\delta \neq 0$. Indeed, let $\mathcal{I}_i$ denote the set of bursters whose interspike frequency equals that of the ith burster; that is, $j \in \mathcal{I}_i$ if and only if $\Omega_j + \sqrt{\varepsilon}\Delta_j = \Omega_i + \sqrt{\varepsilon}\Delta_i$. Then the following near identity change of variables

$$\begin{aligned} z_i = \tilde{z}_i &- \varepsilon \sum_{j \notin \mathcal{I}_i} c_{ij} \int_0^t e^{\mathrm{i}(\Omega_j - \Omega_i + \sqrt{\varepsilon}(\Delta_j - \Delta_i))s} \tilde{z}_j \, ds \\ &- \varepsilon \sum_{j=1}^{n} e_{ij} \int_0^t e^{-\mathrm{i}(\Omega_j + \Omega_i + \sqrt{\varepsilon}(\Delta_j + \Delta_i))s} \bar{\tilde{z}}_j \, ds \end{aligned}$$

transforms the system into

$$\varepsilon^{-1}\dot{z}_i = (b_i u_i + \mathrm{i}\omega_i) z_i + c_i z_i |z_i|^2 - d_i z_i |z_i|^4 + \sum_{j \in \mathcal{I}_i} c_{ij} z_j \ + \ \mathcal{O}(\sqrt[4]{\varepsilon}) \, .$$

For the sake of clarity we write $\sum_{j=1}^{n} c_{ij} z_j$ instead of $\sum_{j \in \mathcal{I}_i} c_{ij} z_j$ and assume that $c_{ij} = 0$ when $j \notin \mathcal{I}_i$. This implies Corollary 4.2.

Finally, we use the same averaging procedure as in the proof of Theorem 2.1 to transform the slow subsystem into the form

$$\varepsilon^{-1}\dot{u}_i = \eta_i (a_i \pm |z_i|^2 \ + \ \mathcal{O}(\sqrt[4]{\varepsilon}))$$

and introduce the slow time $\tau = \varepsilon t$ to obtain the canonical model (4.4). □

Remark 4.5. If the condition C4 is violated, that is, if $y_i \in \mathbb{R}^k$ for some $k > 1$, then u_i, η_i and a_i become complex-valued.

Remark 4.6. If the condition C3 is violated, that is, if $L_{1i}(0) = \mathrm{i}\Lambda_i \neq 0$, then the canonical model has the form

$$\begin{aligned} z_i' &= \mathrm{i}\Lambda_i z_i |z_i|^2 + \sqrt{\varepsilon} \left((b_i u_i + \mathrm{i}\omega_i) z_i + c_i z_i |z_i|^2 - d_i z_i |z_i|^4 + \sum_{j=1}^{n} c_{ij} z_j \right), \\ u_i' &= \sqrt{\varepsilon} \eta_i (a_i \pm |z_i|^2) \end{aligned}$$

plus terms of order $\mathcal{O}(\varepsilon^{3/4})$. Here $' = d/d\tau$, where $\tau = \sqrt{\varepsilon}t$ is the slow time.

Remark 4.7. If $\varepsilon_0 = \mathcal{O}(1)$ in the theorem above, then ε may not be small and the terms hidden in $\mathcal{O}(\sqrt[4]{\varepsilon})$ are not negligible. In this case the burst synchronization mechanism based on the slow passage effect, which we discuss in section 5.2, may never take place. In contrast, if ε is so small that the term $\mathcal{O}(\sqrt[4]{\varepsilon})$ is negligible, then the slow passage effect may play an important role in burst synchronization. We start our analysis of the canonical model by neglecting the term $\mathcal{O}(\sqrt[4]{\varepsilon})$.

5. Synchronization of elliptic bursters. There are two rhythmic processes associated with each burster: repetitive spiking and repetitive bursting. Therefore, there could be at least two different regimes of synchronization; see Figure 5.1.

- Synchronization of individual spikes.
- Synchronization of bursts.

As we will see below, one of them does not imply the other. Therefore, there is an additional regime when both types of synchronization occur simultaneously (see, e.g., Figure 5.2).

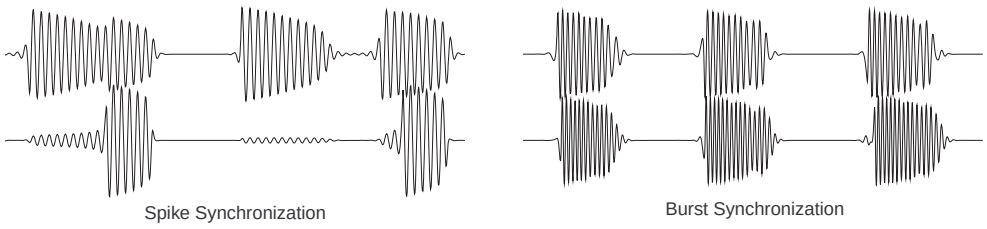

FIG. 5.1. *Various regimes of synchronization of bursters.*

5.1. Spike synchronization. Synchronization of individual spikes within a single burst depends crucially on the interspike frequencies, and in general is difficult to achieve, since the interspike frequencies depend on the amplitudes of spikes $|z_i|$ (via $\operatorname{Im} c_i$ and $\operatorname{Im} d_i$) and the values of the slow variables u_i (via $\operatorname{Im} b_i$).

THEOREM 5.1 (spike synchronization of Bautin bursters). *If in the canonical model* (4.4) *all bursters have equal center frequencies* $\omega_1 = \cdots = \omega_n = \omega$, *the coefficients* b_i, c_i, *and* d_i *are real, and the matrix of synaptic connections* $C = (c_{ij})$ *is self-adjoint, i.e.,* $c_{ij} = \bar{c}_{ji}$, *then the firings of the fast variables* z_i *synchronize on a short time scale of order* 1. *More precisely, activity of the fast subsystem*

$$z_i' = (b_i u_i + \mathrm{i}\omega) z_i + c_i z_i |z_i|^2 - d_i z_i |z_i|^4 + \sum_{j=1}^{n} c_{ij} z_j$$

for $u_i = \text{const}$, $i = 1, \ldots, n$, *converges to a limit cycle.*

Proof. The proof of this theorem is similar to the Cohen–Grossberg convergence theorem for oscillatory neural networks (Hoppensteadt and Izhikevich (1996b), (1997, (Theorem 10.5)).

In the rotating coordinate system

$$w_i(\tau) = e^{-\mathrm{i}\omega\tau} z_i(\tau)$$

the fast subsystem becomes

$$w_i' = b_i u_i w_i + c_i w_i |w_i|^2 - d_i w_i |w_i|^4 + \sum_{j=1}^{n} c_{ij} w_j \ . \tag{5.1}$$

Note that the mapping $U : \mathbb{C}^{2n} \to \mathbb{R}$ given by

$$U(w_1, \ldots, w_n, \bar{w}_1, \ldots, \bar{w}_n) = -\sum_{i=1}^{n} \left(b_i u_i |w_i|^2 + \frac{c_i}{2} |w_i|^4 - \frac{d_i}{6} |w_i|^6 + \sum_{j=1}^{n} c_{ij} \bar{w}_i w_j \right)$$

is a global Liapunov function for (5.1). Indeed, it is continuous, bounded below (because it behaves like $|w|^6$ for large w), and satisfies

$$w_i{}' = -\frac{\partial U}{\partial \bar{w}_i} \ , \qquad \bar{w}_i' = -\frac{\partial U}{\partial w_i} \ ;$$

hence,

$$\frac{dU}{d\tau} = \sum_{i=1}^{n} \left(\frac{\partial U}{\partial w_i} w_i{}' + \frac{\partial U}{\partial \bar{w}_i} \bar{w}_i' \right) = -2 \sum_{i=1}^{n} |w_i{}'|^2 \le 0 \ . \tag{5.2}$$

Notice that $dU/d\tau = 0$ precisely when ${w_1}' = \cdots = {w_n}' = 0$, i.e., at the equilibrium point of (5.1). Let $w^\star \in \mathbb{C}^n$ be such a point. Then, while the solution $w(\tau)$ of (5.1) converges to $w^\star$, the solution of the fast subsystem converges to the limit cycle $z(\tau) = e^{\mathrm{i}\omega\tau} w^\star$.

Whether the spike synchronization is in-phase, anti-phase or just out-of-phase depends on the vector $w^\star \in \mathbb{C}^n$. All possibilities are feasible. □

Remark 5.2. Spike synchronization does not imply burst synchronization. Indeed, the result of the theorem above does not depend on the values of the real parameters b_i, c_i, d_i, and u_i, which could be chosen so that burst synchronization is not achieved.

When we drop the assumption that all $u_i = \text{const}$, then the term

$$\sum_{i=1}^{n} \frac{\partial U}{\partial u_i} {u_i}'$$

appears in (5.2). Since it has order $\eta \ll 1$, it does not affect spike synchronization on a short time scale, but modulates it on a longer time scale of order $1/\eta$.

Now let us discuss spike synchronization when the parameters b_i, c_i, and d_i are allowed to have nonzero imaginary parts. It is convenient to use polar coordinates $z_i = r_i e^{\mathrm{i}\varphi_i}$ and rewrite the fast subsystem in the form

$$r_i' = \operatorname{Re} b_i u_i r_i + \operatorname{Re} c_i r_i^3 - \operatorname{Re} d_i r_i^5 + \sum_{j=1}^{n} s_{ij} r_j \cos(\psi_{ij} + \varphi_j - \varphi_i),$$

$$\varphi_i' = \omega_i + \operatorname{Im} b_i u_i + \operatorname{Im} c_i r_i^2 - \operatorname{Im} d_i r_i^4 + \frac{1}{r_i} \sum_{j=1}^{n} s_{ij} r_j \sin(\psi_{ij} + \varphi_j - \varphi_i),$$

where $s_{ij} = |c_{ij}|$ and $\psi_{ij} = \operatorname{Arg} c_{ij}$; that is, $c_{ij} = s_{ij} e^{\mathrm{i}\psi_{ij}}$. From the last equation we see that $\operatorname{Im} b_i$, $\operatorname{Im} c_i$, and $\operatorname{Im} d_i$ do not play a significant role in spike synchronization when firing of the postsynaptic burster has amplitude smaller than that of the presynaptic ones; that is, when the ratio r_j/r_i is large. If all but one bursters are quiescent, then small amplitude oscillations of fast variables of each quiescent burster are entrained by the large amplitude spiking of the active burster. We could have claimed that there were spike synchronization in this case, except that small amplitude oscillations of fast variables can hardly be called spikes. The situation is subtler when more than one burster is active, since the term

$$\frac{1}{r_i} \sum_{j=1}^{n} s_{ij} r_j \sin(\psi_{ij} + \varphi_j - \varphi_i)$$

may be small even when each ratio r_j/r_i is large. This case is studied elsewhere.

5.2. Burst synchronization. Studying burst synchronization in a network of $n > 2$ Bautin bursters is an important but difficult problem that has not been tackled yet. Even the case of two identical bursters poses many problems, which we do not address in this paper. Instead, we discuss a few obvious facts and leave detailed analysis to the reader.

We distinguish two cases:

- instantaneous burst synchronization via destruction of the slow passage effect,
- burst synchronization via fast threshold modulation.

The first case occurs when each individual burster exhibits slow passage effect; that is, when the system does not have noise and when the small order terms $\mathcal{O}(\sqrt[4]{\varepsilon})$ in the canonical model (4.4) are negligible. The second case covers the rest.

Consider a network of two identical bursters having the term $-|z_i|^2$ in the slow subsystem. Using suitable rescaling of parameters, variables, and time τ, we transform the canonical model (4.4) into the form

$$\begin{aligned} z_i' &= (1+\mathrm{i}\beta)u_i z_i + (2+\mathrm{i}\gamma)z_i|z_i|^2 - (1+\mathrm{i}\sigma)z_i|z_i|^4 + \sum_{j=1}^{n} c_{ij} z_j, \\ u_i' &= \eta(a-|z_i|^2). \end{aligned}$$

We use polar coordinates $z_i = r_i e^{\mathrm{i}\varphi_i}$ to rewrite the system above in the form

$$\begin{aligned} r_i' &= u_i r_i + 2r_i^3 - r_i^5 + \sum_{j=1}^{n} s_{ij} r_j \cos(\psi_{ij} + \varphi_j - \varphi_i), \\ \varphi_i' &= \beta u_i + \gamma r_i^2 - \sigma r_i^4 + \frac{1}{r_i}\sum_{j=1}^{n} s_{ij} r_j \sin(\psi_{ij} + \varphi_j - \varphi_i), \\ u_i' &= \eta(a - r_i^2). \end{aligned}$$

Below we assume that $0 < a < 1$ so that the bursters have behavior with alternating active and silent phase, as in the upper part of Figure 3.1.

Instantaneous synchronization via slow passage effect. One of the most striking features of weakly connected Bautin bursters is that burst synchronization may be achieved almost instantaneously. Let us elaborate. Suppose that both bursters are quiescent, that is, $r_1 \approx 0$ and $r_2 \approx 0$, but the slow variables u_1 and u_2 have different values so that the bursters would start firing at different times if they were uncoupled. Without loss of generality we may assume that $u_1 < u_2$ at the initial moment $t_0 = 0$; see Figure 5.2. Suppose the second burster starts firing, that is, becomes active. After r_2 jumps to the upper branch, activity of the first burster is governed by the system

$$\begin{aligned} r_1' &= u_1 r_1 + 2r_1^3 - r_1^5 + s_{12} r_2 \cos(\psi_{12} + \varphi_2 - \varphi_1), \\ \varphi_1' &= \beta u_1 + \gamma r_1^2 - \sigma r_1^4 + s_{12}\tfrac{r_2}{r_1} \sin(\psi_{12} + \varphi_2 - \varphi_1), \\ u_1' &= \eta(a - r_1^2). \end{aligned}$$

Suppose the first burster continues to be quiescent. Since $r_1 \ll r_2$ in this case, we conclude that

$$\varphi_1(\tau) \to \varphi_2(\tau) + \psi_{12} \tag{5.3}$$

very quickly (hence the term "natural phase difference" for ψ_{12}). Since $\cos(\psi_{12} + \varphi_2(\tau) - \varphi_1(\tau)) \to 1$ with the same rate, the system above reduces to

$$\begin{aligned} r_1' &= u_1 r_1 + 2r_1^3 - r_1^5 + s_{12} r_2, \\ u_1' &= \eta(a - r_1^2). \end{aligned} \tag{5.4}$$

Notice that this system depends only on the synaptic amplitude $s_{12} = |c_{12}| \geq 0$ and does not depend on the natural phase difference $\psi_{12} = \operatorname{Arg} c_{12}$. We combine (5.3) and (5.4) to reach the following conclusion.

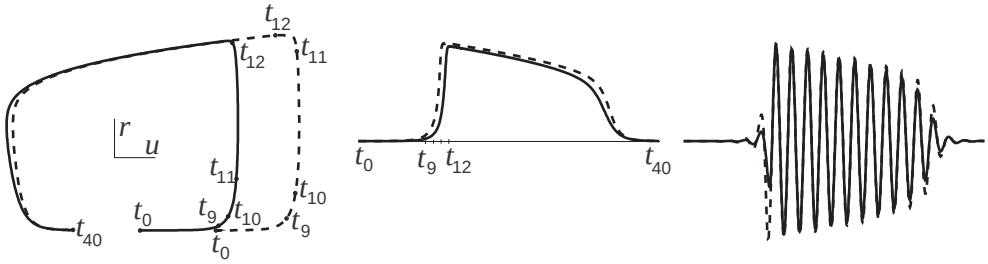

FIG. 5.2. *Two Bautin bursters synchronize almost instantaneously even when they start from essentially different initial conditions. Continuous (dashed) curve is the solution of the first (second) burster. Filled circles denote solutions at the moments* $t_k = k$. *Parameters:* $a = 0.7,\ \eta = 0.1,\ c_{12} = c_{21} = 1/4,\ u_1(0) = -0.3, u_2(0) = -0.25$.

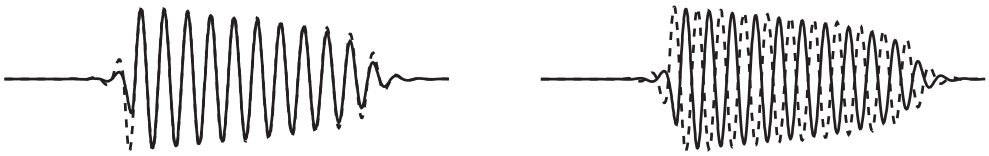

FIG. 5.3. *Illustration to Corollary* 5.3. *Left:* $c_{12} = c_{21} = 1/4$. *Right:* $c_{12} = c_{21} = -1/4$. *Other parameters are as in Figure* 5.2.

COROLLARY 5.3. *Whether connections between local Bautin bursters are excitatory or inhibitory does not affect burst synchronization but affects spike synchronization at least at the onset of a burst; see Figure* 5.3.

Let us contrast the nullclines of the system (5.4) above for $r_2 = 0$ and $r_2 \neq 0$; see Figure 5.4. If the second burster were silent, the nullcline would be N_0 and the first burster would continue to be quiescent due to the slow passage effect depicted in the upper part of Figure 3.1. Since $r_2 \neq 0$, the system above has nullcline of the form N_1. Obviously, r_1 cannot remain near the origin and jumps to the upper branch of N_1 for all values of u_1 greater than certain (negative) value that depends on s_{12}. This process takes $\mathcal{O}(1)$ units of time and looks instantaneous on the larger time scale of order $\mathcal{O}(1/\eta)$ corresponding to the period of each burst. This explains the nearly instantaneous onset of firing by both bursters that we see in Figure 5.2.

In-phase vs. out-of-phase synchronization. Unlike coupled phase oscillators, relaxation oscillators synchronize in-phase even when they have essentially different frequencies. A network of Bautin bursters is not an exception.

Remark 5.4. In-phase synchronization is usually encountered in a network of quantitatively different bursters, whereas out-of-phase synchronization is difficult to achieve.

Indeed, from Figure 5.2 it follows that two bursters synchronize almost instantaneously even when they have essentially different values of slow variables u_1 and u_2. The difference may be due to distinct initial conditions as well as distinct quantitative features. For example, if one of the bursters, say the first one, has a longer interburst period, it tends to fall behind the second burster during the quiescent state even when they start from identical initial conditions. If the quantitative distinction is not too sharp, the first burster would be in the zone of the slow passage effect ($u_1 > 0$) by the time the second burster starts to fire. Since the slow passage effect is sensitive to perturbations, firing of the second burster destroys the effect and elicits almost

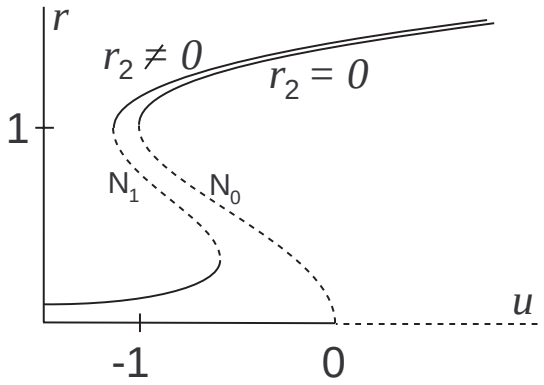

FIG. 5.4. *Nullclines N_0 and N_1 of the system* (5.4) *for $r_2 = 0$ and $r_2 = 1$, respectively (value $s_{12} = 1/8$ was used).*

instantaneous response of the first burster. Even though there is a $\mathcal{O}(1)$ delay in the response, which may be considered as a phase shift, it is negligible on the large time scale $\mathcal{O}(1/\eta)$, since it constitutes only a small ($\eta \ll 1$) fraction of the period of a burst; see the right-hand side of Figure 5.2.

Fast threshold modulation. If there are many simultaneously active bursters in a network, if the small order term $\mathcal{O}(\sqrt[4]{\varepsilon})$ in the canonical model (4.4) is not negligible (see Remark 4.7), or if there is noise in the system, then each nullcline looks qualitatively like N_1 depicted in Figure 5.4, not like N_0. In this case we may treat the bursters as being strongly connected Bonhoeffer–Van der Pol-type relaxation oscillators, which are studied, e.g., by Belair and Holmes (1984), Grasman (1987), Kopell and Somers (1995), Skinner, Kopell, and Marder (1994), Somers and Kopell (1993), (1995), Storti and Rand (1986), and others. In particular, we may use the *fast threshold modulation* theory (Somers and Kopell (1993)) to study the canonical model (4.4).

Whether or not the bursters synchronize in-phase depends on the relative rates of slow variable on the lower and the upper branches of the nullcline N_1. For example, when a is near 0, variable u increases slowly during the silent phase and decreases quickly during the active phase, which leads to the in-phase synchronization via fast threshold modulation. An out-of-phase synchronization is difficult to achieve in this case even when the bursters are quantitatively different. In contrast, when a is near 1, the rate during the active phase may be slower than that during the silent phase, which may lead to desynchronization even when the bursters are identical. These informal considerations can be made precise when $|c_{ij}|$ are not very large (Izhikevich (1999)).

6. FitzHugh–Rinzel model. It should be noted that our analysis was local; that is, the reduction of an arbitrary Bautin burster to the canonical model was proved only in a small neighborhood of the Bautin point. Thus, we may not make any global conclusions without further analysis. In this section we use the FitzHugh–Rinzel model of subcritical elliptic burster (Rinzel (1987)) to evaluate how studying local Bautin bursters contributes to our understanding of global subcritical elliptic bursting.

The FitzHugh–Rinzel model takes the form

$$\dot{v} = v - v^3/3 - w + y + I,$$

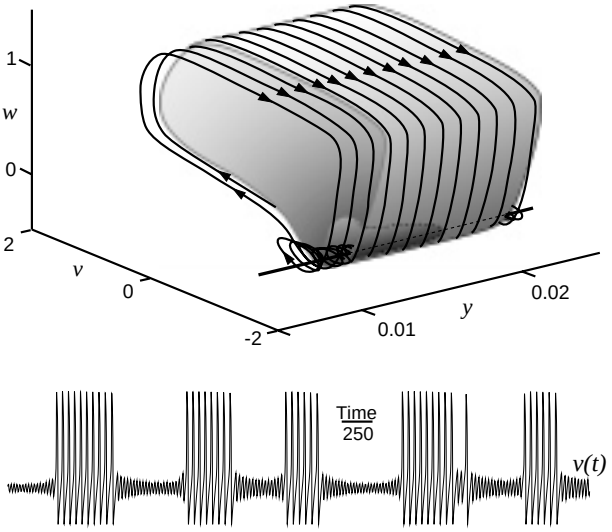

FIG. 6.1. *FitzHugh–Rinzel subcritical elliptic burster.*

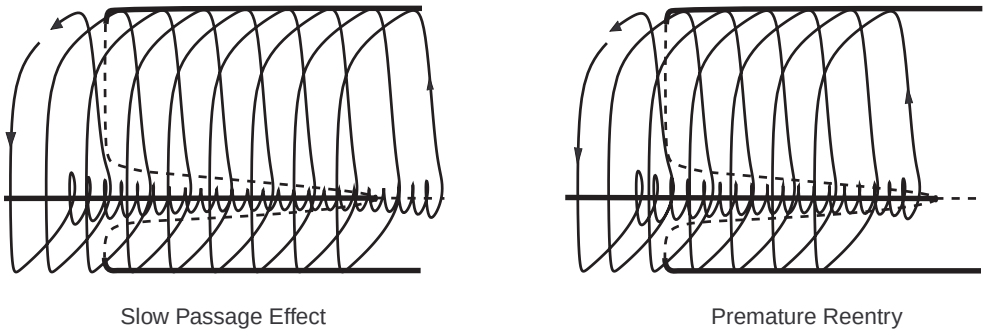

FIG. 6.2. *Slow passage effect and premature reentry into the active phase in the FitzHugh–Rinzel model.*

$$\dot{w} = \delta(a + v - bw),$$
$$\dot{y} = \mu(c - v - dy)$$

where $I = 0.3125,\ a = 0.7,\ b = 0.8,\ c = -0.775,\ d = 1,\ \delta = 0.08$, and $\mu = 0.0001$ are the values used by Rinzel (1987). This system can be written in the form (1.1) if we denote $x = (v, w) \in \mathbb{R}^2$. Note that the fast subsystem is the classical FitzHugh–Nagumo equation (FitzHugh (1961)), which we discussed in section 1.2, see also Figure 6.3, and the slow subsystem is one-dimensional. The FitzHugh–Rinzel model with the parameters defined above produces singular subcritical elliptic bursting with large amplitude spikes; see Figure 6.1. Therefore, one would expect the behavior of the FitzHugh–Rinzel model to be quite different from that of the canonical model (1.4).

Another feature of the FitzHugh–Rinzel model is that the attraction to the unique equilibrium is relatively weak. As was pointed our by Rinzel (1987), this may decrease the slow passage effect or even lead to premature reentry into the active phase; see Figure 6.2. The latter likely contributes to the apparent irregularity of bursting.

We conclude by noting that the FitzHugh–Rinzel model with the choice of the

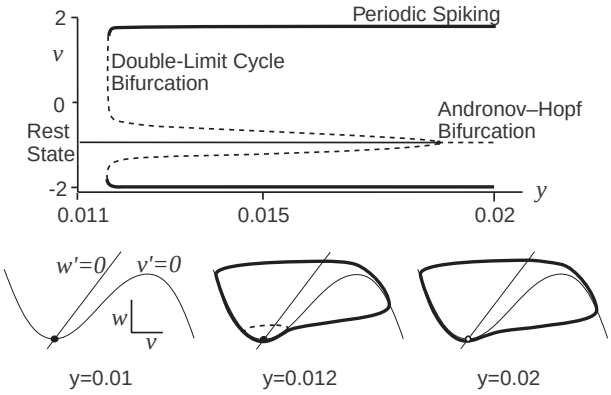

FIG. 6.3. *Bifurcations in the FitzHugh–Rinzel subcritical elliptic burster.*

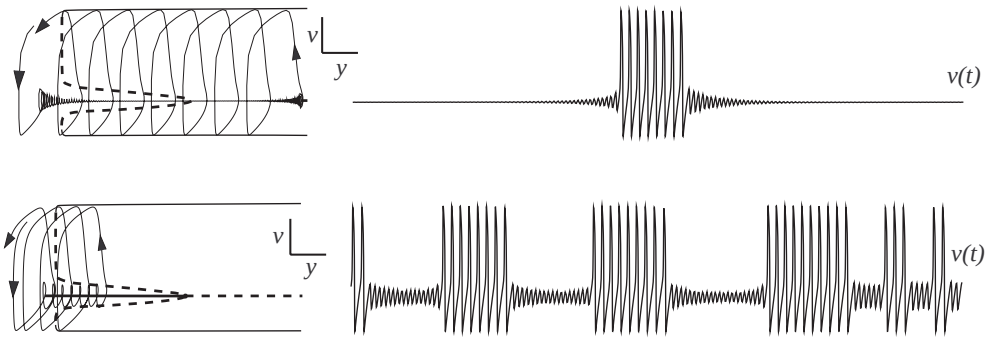

FIG. 6.4. *Solutions of the FitzHugh–Rinzel model for* $c = -0.9$ *(upper part) and* $c = -0.75$ *(lower part).*

parameters above by no means could be classified as local Bautin burster. This sets fair grounds for our comparisons below.

6.1. Onset and termination of bursting. Let us test how studying the canonical model (1.4) contributes to our understanding of subcritical elliptic bursting. In particular, let us compare how periodic bursting appears and disappears when we change parameters of the slow subsystem. Parameter a in the canonical model corresponds (up to a rescaling) to the parameter c in the FitzHugh–Rinzel model. Decreasing of a leads to longer interburst intervals but relatively constant burst duration. Increasing of a leads to shorter interburst intervals until the periodic bursting becomes tonic spiking; see Figure 3.1. Similar behavior is observed in the FitzHugh–Rinzel model and in the Wu–Baer model (1997) with the exception that the transition from periodic bursting to tonic spiking is erratic; see Figure 6.4.

6.2. Spike vs. burst synchronization. Let us consider a network of FitzHugh–Rinzel subcritical elliptic bursters which we take in the form

$$\dot{v}_i = v_i - v_i^3/3 - w_i + y_i + I + \sum_{j=1}^{n} s_{ij} v_j,$$
$$\dot{w}_i = \delta_i(a + v_i - b w_i),$$

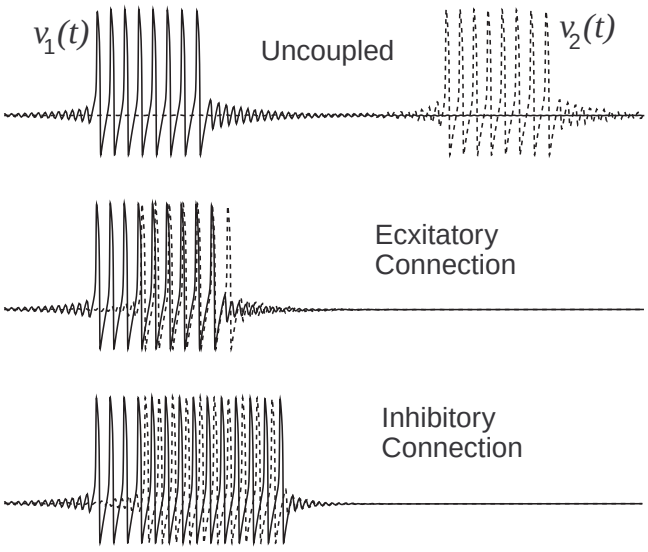

FIG. 6.5. *Solutions of two weakly coupled FitzHugh–Rinzel bursters. Upper part:* $s_{12} = s_{21} = 0$. *Middle part:* $s_{12} = s_{21} = 0.002$. *Lower part:* $s_{12} = s_{21} = -0.002$.

$$\dot{y}_i = \mu(c - v_i - dy_i).$$

Parameters s_{ij} determine the strength and sign of connections between the bursters.

We select $c = -0.9$ so that each burster behaves as depicted in the upper part of Figure 6.4. We use $n = 2$ and such initial conditions that the second burster, if uncoupled from the first one ($s_{21} = 0$), starts to fire with a considerable delay; see the upper part of Figure 6.5. When weakly coupled ($|s_{ij}| = 0.002$), the bursters tend to synchronize regardless of the sign of the connection; see the rest of Figure 6.5. Thus, whether the connections are excitatory or inhibitory does not affect burst synchronization in the FitzHugh–Rinzel model, but affects only spike synchronization. This is in a total agreement with the Corollary 5.3 and the Figure 5.3. A new feature of the FitzHugh–Rinzel model is a considerable prolongation of active phase when the connections are inhibitory. We do not see this in the canonical model.

6.3. FM interactions. To check how interactions between the FitzHugh–Rinzel bursters depend on the relation between their frequencies, we consider a pair of such bursters with $s_{12} = 0$ and $s_{21} = 0.002$. Thus, the first burster is presynaptic and the second one is postsynaptic. We vary parameter δ_1 to control the spiking frequency of the presynaptic burster. The other parameters were unchanged. We chose initial conditions so that the presynaptic burster begins its active phase at time $t = 0$, whereas the postsynaptic one, if uncoupled, becomes active with a substantial delay (more than 1000 units of time).

Since the frequency of large amplitude spiking in a relaxation oscillator differs substantially from the frequency of small amplitude oscillation near the equilibrium, none of the cases depicted in Figure 6.6 corresponds to 1:1 locking. The upper part of the figure corresponds to 1:2 locking; that is, the membrane potential of the postsynaptic burster produces two small amplitude oscillations during each spike of the presynaptic one. Apparently, a few spikes are enough to destabilize the postsynaptic burster and make it active. This is not the case in the second and the third figure

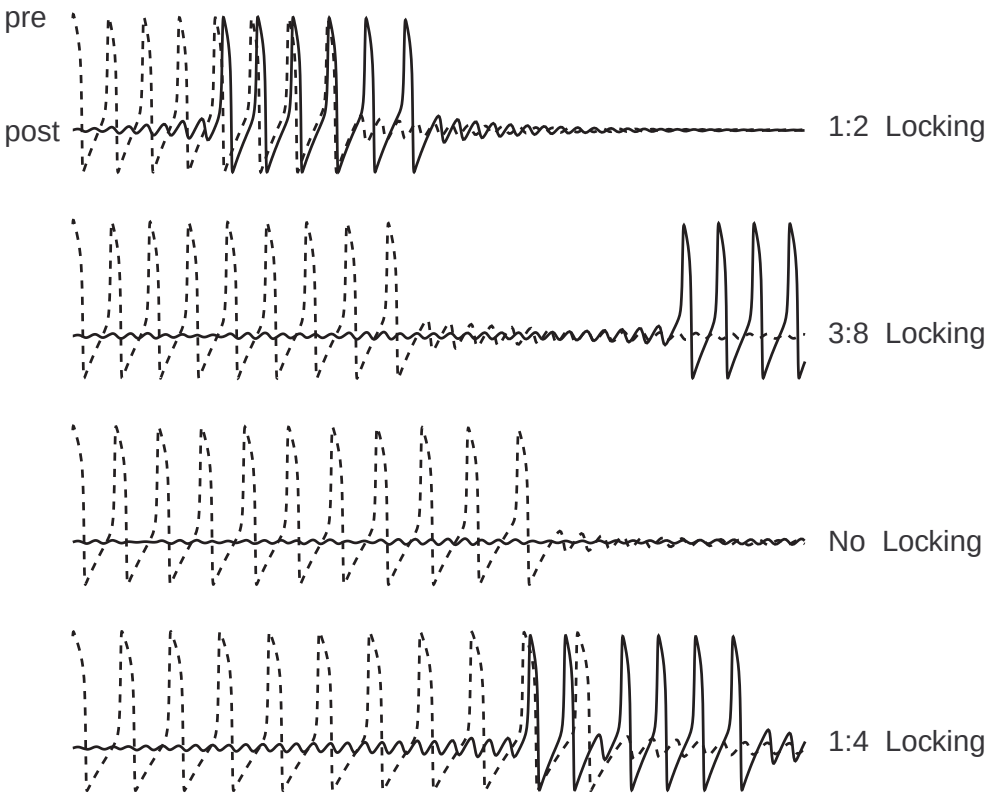

FIG. 6.6. *Frequency modulated (FM) interactions between weakly connected FitzHugh–Rinzel bursters. Parameters:* $I = 0.3125,\ a = 0.7,\ b = 0.8,\ c = -0.9,\ d = 1,\ \mu = 0.0001$, *and* $s_{12} = 0$ *and* $s_{21} = 0.002$. *Simulation time* $t \in [0, 1000]$. *The parameter* δ_1 *was used to control the spiking frequency of the presynaptic burster. From top to the bottom:* $\delta_1 = 0.08,\ 0.07,\ 0.06,\ 0.05$.

from the top, even though the presynaptic neuron generates more spikes. At the bottom we depicted the case of 1:4 locking, which leads to relatively rapid postsynaptic response.

We see that the Corollary 4.2 is not applicable to subcritical elliptic bursters of singular type. A possible explanation would be that local Bautin bursters produce small amplitude spiking, whereas the FitzHugh–Rinzel bursters produce large amplitude spiking. The actual reason is slightly deeper: The limit cycle corresponding to repetitive spiking has circle shape in the former case, but it is distorted in the latter case. Such a distortion generates harmonics and subharmonics, which start to play a role in locking behavior. Similar discrepancies can be observed between weakly connected networks near multiple Andronov–Hopf bifurcation and weakly connected limit cycle (phase) oscillators (Hoppensteadt and Izhikevich (1997)). In order to establish communication, one requires equality of frequencies in the former case, whereas only their resonance is enough in the latter.

Finally, notice an important difference between local Bautin bursters and singular subcritical elliptic bursters: the large amplitude spiking and the small amplitude oscillations near the equilibrium have nearly identical frequencies in the former, but may have drastically different frequencies in the latter. Therefore, we must distinguish the interspike frequency and the frequency of small amplitude membrane oscillations

and state an analogue of Corollary 4.2 in the following form.

Remark 6.1. The rate of burst synchronization of weakly connected subcritical elliptic bursters of singular type depends on the ratio of interspike frequency of the presynaptic burster and the frequency of small amplitude oscillations of the postsynaptic burster. It is fastest when the frequencies are nearly identical, slower when the ratio is near 1:2 or 2:1, even slower for the ratio near 1:3, or 3:1, etc. In contrast, spike synchronization depends on the ratio of interspike frequencies and does not depend on the frequencies of small amplitude oscillations.

7. Discussion. The main purpose of this paper is to derive a canonical model (1.4) for subcritical elliptic bursters of Bautin type.

7.1. Bursters are local. A major requirement for such a derivation is that the bursters are local; that is, the transition to periodic spiking (via Andronov–Hopf bifurcation) and back to quiescent state (via double limit cycle bifurcation) occurs for nearby values of a slow variable. Incidentally, this does not imply that there are only few spikes during each burst; the slow variable changes so slowly that the fast subsystem has enough time to generate many spikes.

We study the case when the fast subsystem is in a small neighborhood of the Bautin bifurcation point where the Andronov–Hopf and double limit cycle bifurcation curves meet. This imposes additional restrictions onto the elliptic bursters that can be transformed into the canonical form (1.4).

A consequence of being near Bautin bifurcation point is that the periodic spiking may have small amplitude. In this case the canonical model captures subcritical elliptic bursting in "embryo." Nevertheless, it does reflect some qualitative features of global subcritical elliptic bursters (see Figure 1.6) provided that no bifurcation occurs while the fast subsystem is pulled out from a small neighborhood of Bautin point.

7.2. Singular vs. nonsingular bursters. An important case that is not covered by our analysis is when the fast subsystem has many time scales and generates spikes via relaxation oscillations. In this case a subcritical elliptic burster may be singular. A typical example of such a burster is the FitzHugh–Rinzel model that we consider in section 6. Computer simulations of the model show that local analysis of Bautin bursters provides accurate insight into global behavior of singular subcritical elliptic bursters.

7.3. Hysteresis. It is remarkable that the slow variable in the canonical model (1.4) is one-dimensional and it oscillates via a hysteresis. Indeed, the slow variable in the original burster (1.1) is multidimensional and our only assumption about the slow dynamics is that it has a stable equilibrium. We do not assume anything about hysteresis, but it seems to emerge naturally during the canonical model derivation. Thus, we come to the conclusion that hysteresis behavior of slow subsystem in subcritical elliptic bursters is a natural property, not an artifact of "minimal" models.

7.4. Biological plausibility. An advantage of studying the canonical model (1.4) is that it is simpler than most of systems of the form (1.1). One may argue that this is not an advantage at all, since

- multidimensional systems of the form (1.1) describing subcritical elliptic bursters are more biologically plausible than the canonical model, because they

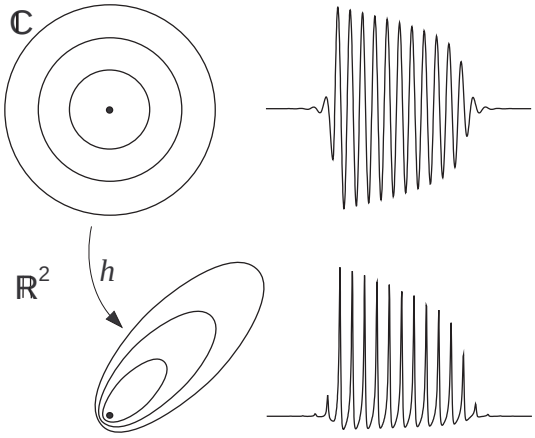

FIG. 7.1. *A homeomorphism $h : C \to \mathbb{R}^2$ may transform solutions of the canonical model to a more "biologically plausible" form. See text for details. (Simulations are performed for $h(z) = z|z|/(1.1|z| - \mathrm{Re}\,(ze^{-\mathrm{i}\pi/4}))$, $a = 0.7$ and $\eta = 0.1$.)*

may take into account many physiological facts, which are hard to identify in (1.4), and

- solutions of the canonical model have simple shape that is different from familiar "Hodgkin–Huxley-type" shape that we see in electrophysiological experiments (contrast the upper and lower part of Figure 7.1).

First of all, each local Bautin burster of the form (1.1) can be transformed into the canonical model by an appropriate *continuous* change of variables (this is the definition of being a canonical model). The form of the canonical model captures the essence of Bautin bursting that is present in all (1.1), while the parameters of the canonical model capture the particulars of each individual burster. The fact that we do not have complete and precise information about all neurophysiological processes taking place during bursting means that we do not know and probably will never know the exact form of the functions f and g in (1.1) (we do not even know the dimension of the vectors x and y), which is frustrating. The same fact in terms of the canonical model means that we do not know the exact values of the parameters a and η, which is much less frustrating since we can study it for all a and η. This is the reason we are interested in canonical models (see the book by Hoppensteadt and Izhikevich (1997) for more examples of canonical models).

Next, notice that any system that is topologically equivalent to the canonical model (1.4) is a canonical model too. Therefore, if one does not like the shape of spiking in (1.4), he could take a homeomorphism $h : \mathbb{C} \to \mathbb{R}^2$ that distorts nice periodic orbits corresponding to repetitive spiking into something less nice but more "biologically plausible." Let $w = h(z)$; then the canonical model is transformed into a system of the form

$$w' = Dh(h^{-1}(w))[(u + \mathrm{i}\omega)h^{-1}(w) + 2h^{-1}(w)|h^{-1}(w)|^2 - h^{-1}(w)|h^{-1}(w)|^4],$$
$$u' = \eta(a - |h^{-1}(w)|^2),$$

which produces spikes of desired shape; see the illustration in Figure 7.1. Its behavior is exactly the same as that of (1.4), since they are topologically equivalent, but the system above is less mathematically tractable.

7.5. Weakly connected networks. When we derive the canonical model for weakly connected Bautin bursters, we do not assume that they are connected exclusively via fast variables; see equation (4.1). Nevertheless, the canonical model (4.4) is connected only via fast variables. Therefore, the connections "fast → slow," "slow → slow," and "slow → fast" can be removed by an appropriate continuous change of variables; see Theorem 4.1. Since the connections "fast → fast" correspond to interaction via spikes, we speculate that even if two bursters could interact via a nonspiking mechanism, it would be much less effective than spiking interaction. Similar conclusions arise in studying weakly connected relaxation oscillators (Hoppensteadt and Izhikevich (1997, section 6.9)).

7.6. Frequency modulated interactions. A seemingly counterintuitive fact is that weakly connected local Bautin bursters do not interact unless they have matching interspike frequencies (Corollary 4.2). That is, synaptic transmission between a pair of bursting neurons having distinct interspike frequencies averages to zero, and hence it is functionally insignificant. Since the significance of interactions between bursters is determined by the interspike frequency, we refer to such interactions as being frequency modulated (FM).

The requirement that the frequencies must coincide is a consequence of the fact that the spiking of presynaptic burster and the small amplitude oscillations near the equilibrium of the postsynaptic burster have circular shape. When the spiking has a distorted shape, as in the FitzHugh–Rinzel model, then the requirement that the frequencies be nearly identical is replaced by the requirement that the frequencies be nicely commensurable (see Hoppensteadt and Izhikevich (1997, Chapter 9)); that is, the interactions are most effective for nearly identical frequencies, less effective when the frequency ratio is near 2:1 or 1:2, even less effective for the ratio 3:1 or 1:3, etc., and negligible when the ratio is near $i : j$ for some large relatively prime integers i and j. Here "near" means ε-close, where $\varepsilon \ll 1$ is the strength of connections.

This result is no longer counterintuitive if we recall how the slow passage effect can be affected by noise. Baer, Erneux, and Rinzel (1989) showed that the noise reduces the slow passage effect through resonance; that is, the noise should have frequencies in its power spectrum that are integer multiples of the natural frequency Ω at the Andronov–Hopf bifurcation; see remark in section 3.2. If we treat a weak input to a burster as a noise, then it is clear that the input is functionally insignificant unless it has resonant frequencies. Llinás (1988) suggested to use the term *resonator* for such FM interacting neurons.

An important difference between local Bautin bursters and (global) subcritical elliptic bursters is that the spiking and the small amplitude oscillations near the equilibrium have nearly identical frequencies in the former but may have drastically different frequencies in the latter. As a result, we have to be more specific when we compare frequencies of oscillations of (global) subcritical elliptic bursters. For example, burst synchronization depends on the ratio of interspike frequency of presynaptic burster and the frequency of small amplitude (subthreshold) oscillations of the postsynaptic one. In contrast, spike synchronization depends exclusively on the ratio of interspike frequencies.

7.7. Rate of synchronization. The rate of convergence to attractors in weakly connected networks is very slow; namely, it is of order $\varepsilon \ll 1$, where ε is the strength of connections (Hoppensteadt and Izhikevich (1997)). For example, a weakly connected

oscillatory network needs as many as $\mathcal{O}(1/\varepsilon)$ cycles to synchronize[1] regardless of whether each element is a relaxation oscillator or a phase (limit cycle) oscillator. This is the major source of criticism of weakly connected models, since the slow rate of convergence contradicts the *CPG* behavior in the lamprey, which is characterized by a strong rate of convergence to attractor (see, e.g., Kopell (1995), Somers and Kopell (1995), Williams and Sigvardt (1995)).

Our analysis of weakly connected bursters suggests that the discrepancy in rates of convergence is not due to the assumption of weakness of connections, but due to the assumption that each segment of lamprey spinal cord can be modeled by an oscillator. If we model it by a burster, which it is, then the rate of convergence to an attractor looks "fast" compared to the interburst period despite the fact that the bursters are weakly connected. Indeed, it takes $\mathcal{O}(1/\varepsilon)$ spikes to produce $\mathcal{O}(1)$ changes in the activity of a postsynaptic segment, but there are as many as $\mathcal{O}(1/(\varepsilon\eta))$ spikes in each burst. Therefore, one burst is usually enough for two segments to lock. Another way to explain this is to note that locking of two segments requires $\mathcal{O}(1/\varepsilon)$ units of time, but each burst lasts $\mathcal{O}(1/(\varepsilon\eta))$ units. Therefore, locking of segments looks instantaneous on the time scale of interburst intervals, even though it takes the same $\mathcal{O}(1/\varepsilon)$ time to achieve.

We see that the apparent difference in convergence rates of weakly connected limit-cycle oscillators and bursters is a matter of semantics since the former is compared with the inter*spike* intervals whereas the latter is compared with the inter*burst* intervals.

7.8. Spike vs. burst synchronization. We see that it is important to distinguish two rhythmic processes: periodic spiking and periodic bursting. Therefore, there are at least two regimes of synchronization; see Figure 5.1. Spike synchronization is difficult to achieve unless some additional conditions are imposed, e.g., those in Theorem 5.1. In contrast, burst synchronization is difficult to avoid. Moreover, substantial changes in parameters of the system, which would lead to disappearance of synchronization or at least to a considerable phase shift if we modeled weakly connected limit cycle (phase) oscillators, do not produce any significant lag between bursts. That is, burst synchronization tends to be in-phase despite any quantitative differences between the bursters. In this sense, behavior of weakly connected local Bautin bursters resembles that of *strongly connected* relaxation oscillators, as described by Somers and Kopell (1993), (1995).

An odd feature of weakly connected elliptic bursters is that both excitatory and inhibitory synaptic connections lead to in-phase burst synchronization. The sign of the synapse affects only the spike synchronization, i.e., whether it is in-phase, anti-phase or just out-of-phase (see Corollary 5.3), but seems to be irrelevant to bursts synchronization.

Acknowledgments. The author would like to acknowledge Frank Hoppensteadt, whose collaboration and constant support have been invaluable during the last five years. This paper was conceived during a meeting with Thomas Erneux in Snowbird, Utah. Bard Ermentrout pointed out the importance of distinguishing spike and burst synchronization. Many discussions with Steve Baer helped to improve the quality of

[1] By synchronization we mean here convergence to a small but finite neighborhood of an appropriate attractor, which takes $\mathcal{O}(1)$ units of slow time τ and/or $\mathcal{O}(1/\varepsilon)$ units of normal time t. Complete convergence to the attractor is an asymptotic process that requires infinite amount of time, unless the system is non-Lipchitz or the initial state is on the attractor.

the manuscript. In particular, he suggested using the FitzHugh–Rinzel model. Special thanks also goes to Arthur Sherman who made an excellent choice of peer reviewers whose criticism and suggestions helped to improve the quality of the manuscript.

REFERENCES

V.I. Arnold, V.S. Afrajmovich, Yu.S. Il'yashenko, and L.P. Shil'nikov (1994), *Bifurcation theory*, in Dynamical Systems V. Bifurcation Theory and Catastrophe Theory, V.I. Arnold, ed.Springer-Verlag, New York.

S.M. Baer and T. Erneux (1986), *Singular Hopf bifurcation to relaxation oscillations*, SIAM J. Appl. Math., 46, pp. 721–739.

S.M. Baer and T. Erneux (1992), *Singular Hopf bifurcation to relaxation oscillations* II, SIAM J. Appl. Math., 52, pp. 1651–1664.

S.M. Baer, T. Erneux, and J. Rinzel (1989), *The slow passage through a Hopf bifurcation: Delay, memory effects, and resonances*, SIAM J. Appl. Math., 49, pp. 55–71.

J. Belair and P. Holmes (1984), *On linearly coupled relaxation oscillations*, Quart. Appl. Math, 42, pp. 193–219.

R. Bertram, M.J. Butte, T. Kiemel, and A. Sherman (1995), *Topological and phenomenological classification of bursting oscillations*, Bulletin of Mathematical Biology, 57, pp. 413–439.

R.M. Borisyuk and A.B. Kirillov (1992), *Bifurcation analysis of a neural network model*, Biological Cybernetics, 66, pp. 319–325.

W. Eckhaus (1983), *Relaxation oscillations including a standard chase of French ducks*, in Asymptotic Analysis II, Lecture Notes in Math. 985, pp. 432–449.

G.B. Ermentrout and N. Kopell (1986a), *Parabolic bursting in an excitable system coupled with a slow oscillation*, SIAM J. Appl. Math., 46, pp. 233–253.

G.B. Ermentrout and N. Kopell (1986b), *Subcellular oscillations and bursting*, Math. Biosci., 78, pp. 265–291.

N. Fenichel (1971), *Persistence and smoothness of invariant manifolds for flows*, Indiana Univ. Math. J., 21, pp. 193–225.

R. FitzHugh (1961), *Impulses and physiological states in models of nerve membrane*, Biophysics Journal, 1, pp. 445–466.

J. Grasman (1987), *Asymptotic Methods for Relaxation Oscillations and Applications*, Springer-Verlag, New York.

J. Guckenheimer and D. Holmes (1983), *Nonlinear Oscillations, Dynamical Systems, and Bifurcations of Vector Fields*, Springer-Verlag, New York.

L. Holden and T. Erneux (1993a), *Slow passage through a Hopf bifurcation: From oscillatory to steady state solutions*, SIAM J. Appl. Math., 53, pp. 1045–1058.

L. Holden and T. Erneux (1993b), *Understanding bursting oscillations as periodic slow passages through bifurcation and limit points*, J. Math. Biol., 31, pp. 351–365.

F.C. Hoppensteadt and E.M. Izhikevich (1997), *Weakly Connected Neural Networks*, Springer-Verlag, New York.

F.C. Hoppensteadt and E.M. Izhikevich (1998), *Thalamo-cortical interactions modeled by weakly connected oscillators: Could brain use FM radio principles?*, BioSystems, 48, pp. 85–94.

F.C. Hoppensteadt and E.M. Izhikevich (1996a), *Synaptic organizations and dynamical properties of weakly connected neural oscillators:* I. *Analysis of canonical model*, Biological Cybernetics, 75, pp. 117–127.

F.C. Hoppensteadt and E.M. Izhikevich (1996b), *Synaptic organizations and dynamical properties of weakly connected neural oscillators.* II. *Learning of phase information*, Biological Cybernetics, 75, pp. 129–135.

E.M. Izhikevich (1998), *Supercritical Elliptic Bursting and the Slow Passage Effect*, preprint.

E.M. Izhikevich (1999), *Phase equations for relaxation oscillators*, SIAM J. Appl. Math., in press.

E.M. Izhikevich (2000), *Neural excitability, spiking, and bursting*, Int. J. Bifurcation and Chaos, 10, in press.

N. Kopell (1995), *Chains of coupled oscillators*, in Brain Theory and Neural Networks, M.A. Arbib, ed., MIT Press, Cambridge, MA.

N. Kopell and D. Somers (1995), *Anti-phase solutions in relaxation oscillators coupled through excitatory interactions*, J. Math. Biol., 33, pp. 261–280.

Yu. Kuznetsov (1995), *Elements of Applied Bifurcation Theory*, Springer-Verlag, New York.

R.R. Llinás (1988), *The intrinsic electrophysiological properties of mammalian neurons: Insights into central nervous system function*, Science, 242, pp. 1654–1664.

A. Mason, A. Nicoll, and K. Stratford (1991), *Synaptic transmission between individual pyramidal neurons of the rat visual cortex* in vitro, The Journal of Neuroscience, 11, pp. 72–84.

B.L. McNaughton, C.A. Barnes, and P. Andersen (1981), *Synaptic efficacy and EPSP summation in granule cells of rat fascia dentata studied in vitro*, Journal of Neurophysiology, 46, pp. 952–966.

A. Nejshtadt (1985), *Asymptotic investigation of the loss of stability by an equilibrium as a pair of eigenvalues slowly cross the imaginary axis*, Uspekhi. Mat. Nauk, 40, pp. 190–191.

J. Rinzel (1987), *A formal classification of bursting mechanisms in excitable systems*, in Mathematical Topics in Population Biology, Morphogenesis, and Neurosciences, Lecture Notes in Biomath. 71, E. Teramoto, M. Yamaguti, eds., Springer-Verlag, Berlin.

J. Rinzel and Y.S. Lee (1987), *Dissection of a model for neuronal parabolic bursting*, J. Math. Biol., 25, pp. 653–675.

R.J. Sayer, M.J. Friedlander, and S.J. Redman (1990), *The time course and amplitude of EPSPs evoked at synapses between pairs of CA3/CA1 neurons in the hippocampal slice*, Journal Neuroscience, 10, pp. 826–836.

F.K. Skinner, N. Kopell, and E. Marder (1994), *Mechanism for oscillations and frequency control in reciprocally inhibitory model neural networks*, Journal of Computational Neuroscience, 1, pp. 69–87.

D. Somers and N. Kopell (1993), *Rapid synchronization through fast threshold modulation*, Biological Cybernetics 68, pp. 393–407.

D. Somers and N. Kopell (1995), *Waves and synchrony in networks of oscillators or relaxation and non-relaxation type*, Phys. D, 89, pp. 169–183.

D.W. Storti and R.H. Rand (1986), *Dynamics of two strongly coupled relaxation oscillators*, SIAM J. Appl. Math., 46, pp. 56–67.

X.J. Wang and J. Rinzel (1995), *Oscillatory and bursting properties of neurons*, in Brain Theory and Neural Networks, M.A. Arbib, ed., MIT Press, Cambridge, MA.

T.L. Williams and K.A. Sigvardt (1995), *Spinal cord of lamprey: Generation of locomotor patterns*, in Brain Theory and Neural Networks, M.A. Arbib, ed., MIT Press, Cambridge, MA.

H.-Y. Wu and S.M. Baer (1997), *Analysis of an Excitable Dendritic Spine with an Activity-Dependent Stem Conductance*, J. Math. Biol., 36, pp. 569–592.